Global Change Biology Communications

WILEY

Global Change Biology Communications
BIOLOGY FOR A RAPIDLY CHANGING WORLD

RESEARCH ARTICLE OPEN ACCESS

Projected Warming of the Southern Ocean Disrupts Embryonic Development and Hatch Timing in Antarctic Fish

Margaret Streeter[1,2] | Nathalie R. Le François[3] | Thomas Desvignes[4,5] | Jacob Grondin[2] | John H. Postlethwait[4] | H. William Detrich III[2] | Jacob M. Daane[1]

[1]Department of Biology and Biochemistry, University of Houston, Houston, Texas, USA | [2]Department of Marine and Environmental Sciences, Marine Science Center, Northeastern University, Nahant, Massachusetts, USA | [3]Laboratoire de Physiologie, Aquaculture et Conservation, Biodôme de Montréal/Espace Pour la Vie, Montréal, Québec, Canada | [4]Institute of Neuroscience, University of Oregon, Eugene, Oregon, USA | [5]Department of Biology, University of Alabama at Birmingham, Birmingham, Alabama, USA

Correspondence: Jacob M. Daane (jdaane@uh.edu)

Received: 10 December 2025 | **Revised:** 12 December 2025 | **Accepted:** 30 December 2025

Keywords: Antarctica | climate change | embryonic development | fish

ABSTRACT

Rising ocean temperatures pose significant threats to marine ectotherms. Sensitivity to temperature varies across life stages, with embryos often being less tolerant to thermal perturbation than adults. Antarctic notothenioid fishes evolved to occupy a narrow, cold thermal regime (−2 to +2°C) as the high-latitude Southern Ocean (SO) cooled to its present icy temperatures, and they are particularly vulnerable to small temperature changes, which makes them sentinel species for assessing climate change impacts. Here, we detail how predicted warming of the SO may affect embryonic development in the Antarctic bullhead notothen, *Notothenia coriiceps*. Experimental embryos were incubated at +4°C, a temperature projected for the SO within the next 100–200 years under high-emission climate models, whereas control embryos were incubated at present-day ambient temperature, ~0°C. Elevated temperature caused a high incidence of embryonic morphological abnormalities, including body-axis curvature and reduced length. Experimental embryos also developed more rapidly, hatching 68 days earlier than controls (87 vs. 155 days post-fertilization). Accelerated development disrupted the timing of seasonal hatching, shifting larval emergence into the polar winter when food is scarce. Transcriptomic analyses revealed molecular signatures of hypoxia and disrupted protein folding in near-hatching embryos, indicating severe cellular stress. Predictive modeling suggested that temperature-induced developmental disruptions would narrow seasonal reproductive windows, thereby threatening population viability under future climate scenarios. Our findings underscore the vulnerability of Antarctic fish embryos to higher water temperature and highlight the urgent need to understand the consequences of disruption of this important trophic component on ecosystem stability in the SO.

1 | Introduction

Although the Southern Ocean (SO) has historically been one of the most thermally stable marine habitats, it is projected to experience dramatic environmental changes (Intergovernmental Panel on Climate Change (IPCC) 2022). Between 2005 and 2017, the SO absorbed 45%–62% of global ocean heat despite covering only about 25% of the ocean surface (IPCC 2022). Sea surface temperatures along the West Antarctic Peninsula have risen by 1°C since 1955 (Meredith and King 2005), with projections suggesting an additional warming of 3°C–4°C within the next 100–200 years under high-emission scenarios (SSP5-8.5; Figure 1A)

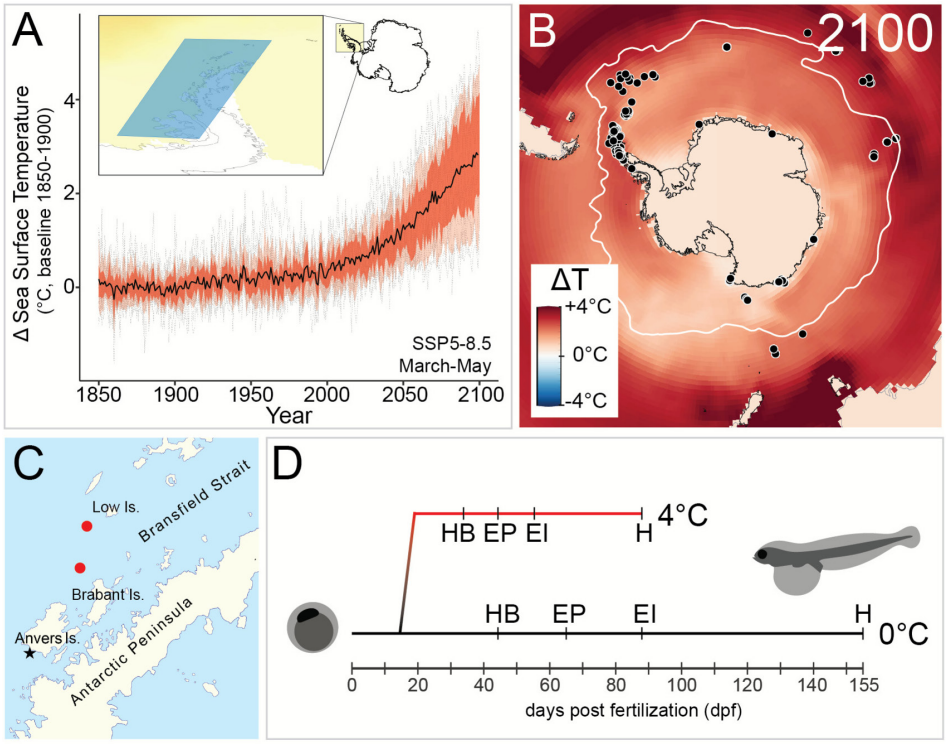

FIGURE 1 | Southern Ocean (SO) warming and *Notothenia coriiceps* embryonic development. (A) Projected change in sea surface temperature (SST) along the Antarctic peninsula (inset) by 2100 and during *N. coriiceps* breeding season (March–May) under the SSP5-8.5 scenario, based on the CMIP6 dataset accessed via the Copernicus Interactive Climate Atlas (Swart et al. 2019). The blue polygon reflects the specific area assessed for change in sea surface temperature. The black line indicates median SST projection, while the gray lines indicate individual climate models. Red and pink shading reflect 25–75th and 10–90th percentiles, respectively. (B) Projected SST changes in the SO under SSP5-8.5 in 2100, overlaid with historical *N. coriiceps* catch records (black dots) from AquaMaps (Ready et al. 2010). Temperature heatmap from the IPCC Interactive Climate Atlas (Iturbide et al. 2022). The white line shows the approximate location of the Antarctic polar front, adapted from (Orsi et al. 1995). (C) Fishing sites at which *N. coriiceps* specimens used in this study were collected (red dots) and the location of Palmer Station, where embryos were raised in the Palmer Station Aquarium in tanks supplied with flow-through seawater from neighboring Arthur Harbor (black star). (D) Developmental timeline of embryos incubated under ambient (0°C) and elevated (4°C) temperatures, highlighting stages selected for RNA sequencing: HB (heartbeat), EP (50% eye pigmentation), EI (eye iridescence), and H (first hatching).

(Swart et al. 2019). Moreover, Antarctic sea ice cover has rapidly declined since its recent peak in 2014, losing as much ice in 3 years as the Arctic did over three decades, indicating a shift toward a new and warmer climate regime (Eayrs et al. 2021; Hobbs et al. 2024). Understanding the impact of these changes on Antarctic marine organisms is crucial for forecasting future ecosystem dynamics.

The ichthyofauna of the modern SO is dominated by species of the Notothenioidei suborder (order Perciformes) (Eastman 2005). Before the mid-Miocene, Antarctic fish biodiversity significantly decreased along with the cooling and glaciation of Antarctica, leading to local extinction of most fish taxa (Eastman 2005). With competition reduced, the benthic common ancestor of notothenioids radiated adaptively about 10 million years ago to yield over 100 species that exploit all niches in the SO (Eastman 2005; Eastman and Eakin 2021; Daane and Detrich 2022; Bista et al. 2023). Today, notothenioids constitute about 90% of fish biomass on the High Antarctic continental shelf, 66.5% of species captured in the Scotia Sea, and include keystone species that are essential for maintaining ecosystem function (Eastman 2005; Liu et al. 2024; Corso et al. 2022; Permitin 1977; Gon and Heemstra 1990).

Persistently cold SO temperatures (−2°C to +2°C annually; Hersbach et al. 2020) contributed to specialized biochemical, cellular, and physiological traits in notothenioids, including antifreeze glycoproteins, loss of red blood cells in icefishes, and absence of a typical heat shock response (Daane and Detrich 2022; Devries 2020; Sidell and O'Brien 2006). These and other cold specializations, however, contribute to narrow thermal tolerances in adults and limit their capacity to cope with thermal stress (Dahlke, Wohlrab, et al. 2020; Bilyk and Devries 2011; Somero and DeVries 1967). While much research has focused on the responses of adult notothenioids to future warming (Bilyk et al. 2018; Beers and Jayasundara 2015; Saravia et al. 2021; O'Brien et al. 2021; Egginton et al. 2019), the effects of elevated temperatures on other life stages, especially embryos, remain poorly understood.

Thermal resilience varies throughout a fish's life cycle, with spawning adults and embryos often exhibiting the lowest

tolerance ranges (Dahlke, Wohlrab, et al. 2020). Temperature has pleiotropic effects on embryos by influencing the kinetics of biochemical reactions, metabolic rates, protein folding and stability, oxidative stress, and sex determination (Irvine 2020). Because the responses of different cell types to thermal stress vary, developmental asynchronies and teratological effects may occur (Dorrity et al. 2023). Furthermore, thermal stress can redirect limited yolk resources away from growth and development toward fueling cellular stress responses, resulting in stunted growth and reduced larval fitness (Sokolova 2021; Réalis-Doyelle et al. 2016; Kamler 2012).

Depending on the climate scenario, an estimated 10%–60% of all fish species are projected to exceed their embryonic developmental temperature limits within their current ranges by 2100 (Dahlke, Wohlrab, et al. 2020). However, experimental data on thermal tolerance limits are scarce for most fish embryos, making it difficult to accurately model the effects of future climate change across diverse fish lineages. The buoyant embryos of several notothenioid species may be particularly vulnerable to thermal stress because, in the absence of sea ice, they are exposed to environmental fluctuations near the sea surface (La Mesa et al. 2021). Previous studies of Antarctic embryo thermal resilience are sparse and limited to short-term thermal exposures of field-collected embryos from a single Antarctic dragonfish species (*Gymnodraco acuticeps*, Bathydraconidae) (Flynn et al. 2015; Flynn and Todgham 2018). Temperature effects on developmental viability varied from limited to strong, potentially due to the timing of heating or other variables (Flynn et al. 2015; Flynn and Todgham 2018).

In the present study, we examine the development of the Antarctic bullhead notothen, *Notothenia coriiceps*, in the context of projected SO warming over the next 100–200 years. We show that increased temperature during embryonic development shortens the time to hatching, causes morphological abnormalities, impacts the phenology of hatching, and perturbs gene expression related to hypoxia, protein homeostasis, and the cellular stress response. Using these insights, we predict a reduction in seasonal embryonic survival and larval recruitment with potential shifts in the timing of breeding.

2 | Results

2.1 | Development of *N. coriiceps* Embryos Under Rising Ocean Temperatures

For environmental conditions, we chose 4°C, predicted to be reached by 2100–2200 given the unmitigated climate emission scenario Shared Socioeconomic Pathways (SSP5-8.5) (IPCC 2022; Swart et al. 2019; Gidden et al. 2019) (Figure 1A). We focused on the Antarctic bullhead notothen, *Notothenia coriiceps*, an abundant species (Figure 1B; Barrera-Oro et al. 2000) with a known breeding season and an established developmental staging series (Postlethwait et al. 2016; Calì et al. 2017). Although *N. coriiceps* adults are benthic (Calì et al. 2017), their zygotes are buoyant, form part of the zooplankton, and are exposed to changing regional sea surface temperatures; thus *N. coriiceps* serves as an excellent proxy for multiple notothenioid species with pelagic embryos (Postlethwait et al. 2016; Kellermann 1991).

Eighty adult *N. coriiceps* were collected during their Austral fall breeding season from two locations along the Antarctic peninsula (Figure 1C; see Section 4). After transport to the aquarium facilities at Palmer Station, Antarctica, fish were maintained in flow-through seawater aquaria at ~0°C. Males and gravid females were injected with Ovaprim, a gonadotropin-releasing hormone analog, to stimulate ovulation and spermiation. Four spontaneous group-spawning events, over 3 days (5/25–5/27/2018) in two 2.5-m^3 circular tanks (30 fish/tank), produced approximately 44,000 embryos. Spawning most likely involved mixed parentage as multiple males and females could have released gametes. Embryos from these four group spawns were pooled, divided into two equivalent technical replicate groups, and incubated at the ambient water temperature of Arthur Harbor (controls, ~0°C). On day 15 post-fertilization, corresponding to ~40% epiboly, each replicate group was split to give one cohort to be incubated at +4°C (experimental) and one (control) at ambient temperature (Figure 1D, Figures S1 and S2). To avoid abrupt heat shock to the embryos, we applied a temperature ramp of ~1°C/day to the two experimental replicates over days 15–19 to increase long-term survival chances (Figure S3 shows the temperature profiles measured for experimental and control incubators). The delayed ramp was intended to mitigate the role of maternal effects on our results. We estimate that the maternal-to-zygotic transition in *N. coriiceps* embryos occurred between 5 and 9 dpf based on cell number, the change to asynchronous and uneven cell division, and the onset of epiboly in early gastrulation (Postlethwait et al. 2016), as found in other fish species (Vastenhouw et al. 2019). Thus, our findings reflect the impact of warming on transcription of the zygotic genome.

The survival rates of embryos were similar between treatments, with the exception of an early mortality event (37.9% mortality over the first 40 days) in one of the ambient technical replicates (Figure S4A,B) that may have resulted from a decline in water quality due to accumulation of dead embryos. Subsequently, embryonic survival at 4°C at 74 dpf was 93.2% and 92.8% for the two heated replicates, compared to 96.3% and 93.1% for the 0°C ambient replicates at 118 dpf (Figure S4B). These results indicated that differential mortality across treatments was unlikely to affect the results reported below.

2.2 | Accelerated Development of *N. coriiceps* Embryos Led to Hatching During Austral Polar Winter

During the 15-day incubation at 0°C, embryos in the four cohorts progressed through cleavage, epiboly, and establishment of the embryonic axis on the *N. coriiceps* staging series (Kamler 2012) (data not shown). Following the temperature ramp up, control and experimental embryos completed gastrulation, segmentation, organogenesis, and entered skeletogenesis prior to hatching, but those at 4°C attained these milestones earlier (Figures 1D and 2A–E, Figure S5). Segmentation in experimental embryos began at 20 dpf at 4°C versus 23 dpf

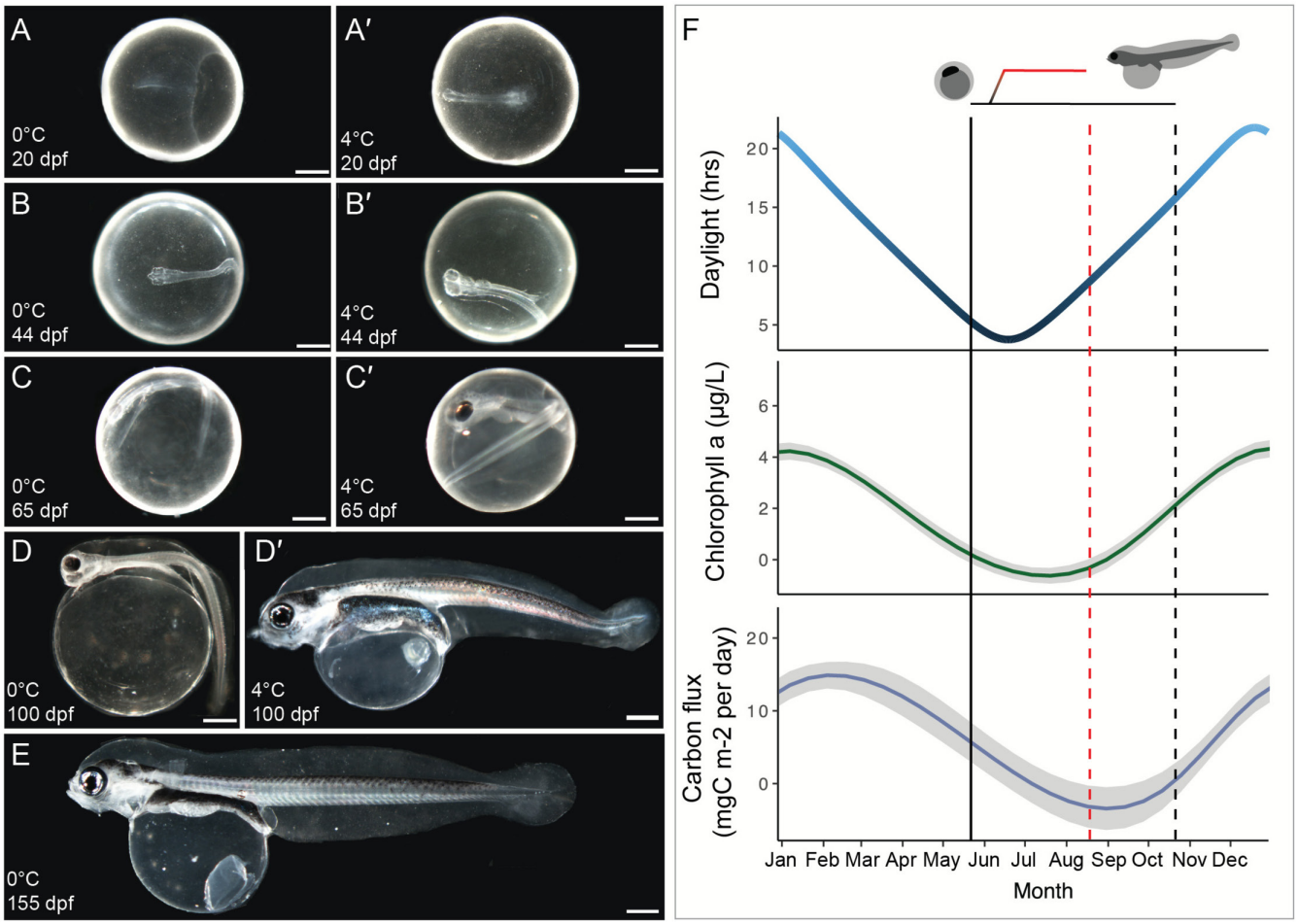

FIGURE 2 | Accelerated developmental rate and phenological asynchrony in *N. coriiceps* embryos raised at elevated temperature. Developmental progression of *N. coriiceps* embryos from 20 days post-fertilization (dpf) to hatching at 0°C (A–E) or at 4°C (A′–D′). Scale bars represent 1 mm. (F) Comparison of relative hatch timing in *N. coriiceps* at 0°C (black dashed line) and 4°C (red dashed line), overlaid with environmental data from the Palmer Station Long-Term Ecological Research (LTER) database on Anvers Island for chlorophyll *a* and carbon flux (Smith et al. 1995; Ducklow and Lter 2014; Palmer Station Antarctica and Schofield 2025). The chlorophyll *a* dataset is condensed from 30 years of measurements, and the carbon flux data comprises 20 years of sediment trap data (gray areas represent confidence bands of localized regression (loess, geom_smooth())). The vertical black solid line represents the day of fertilization for the embryos in this experiment.

at 0°C, first heartbeat occurred at 34 dpf at 4°C compared to 44 days for controls, and the onset of retinal pigmentation and eye iridescence for the experimentals appeared at 44 and 55 dpf, versus 65 and 87 dpf for controls (Figure S5; Table S1). Thus, development of *N. coriiceps* embryos was substantially accelerated at 4°C compared to ambient temperature, but embryos in both treatments nonetheless passed through the same developmental stages.

Control embryos just began hatching at 155 dpf but had not yet reached a peak prior to the conclusion of the field season, which coincided with the onset of hatching (Figure 2E). In contrast, embryos raised at +4°C began hatching at 87 dpf, and hatching continued through 100 dpf (Figure 2D′). Thus, hatching of experimental embryos was completed at least 55 days earlier compared to first hatching of controls. This phenological asynchrony has important implications for post-hatching larval survival and development: hatching of controls at 155 dpf coincides with the arrival of polar spring (November), when food availability increases along the Antarctic Peninsula (Figure 2F; see carbon flux west of Anvers Island and chlorophyll *a* for Arthur Harbor at Palmer Station (Smith et al. 1995; Ducklow and Lter 2014; Palmer Station Antarctica and Schofield 2025)), whereas experimental larvae would hatch in late winter (August–September), a period of low light, low primary productivity and comparatively limited food availability (Iken et al. 1997).

2.3 | Development at 4°C Resulted in Morphological Abnormalities in Larval Stages

Embryos raised at 4°C exhibited several gross morphological abnormalities. Approximately 65% of randomly sampled, near-hatching embryos showed abnormalities at 4°C, compared to only 20% at 0°C (Figure 3A–F, Table S2). The abnormalities included increased body-axis curvature and deformation (Figure 3C), which are phenotypes previously observed in fish embryos under thermal stress (Dorrity et al. 2023), and craniofacial abnormalities involving the jaw (Figure 3D,E). The most

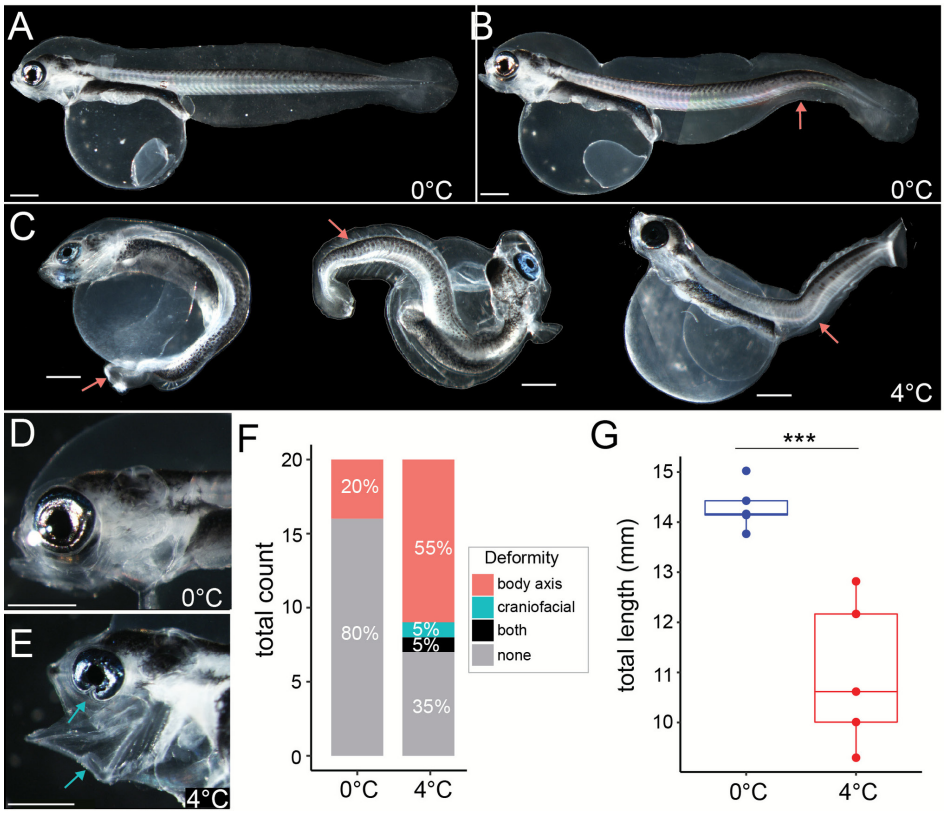

FIGURE 3 | Elevated rates of morphological abnormalities in *N. coriiceps* embryos developing at 4°C. (A) A recently hatched larva developed at 0°C showing normal morphology. (B) An example of an abnormal larva raised at 0°C with body-axis curvature. Arrow pointing to curvature. (C) Examples of abnormalities at hatching-stage embryos raised at 4°C. Scale bars in (A–C) represent 1 mm and arrows point to specific abnormalities including a failure of the axis to fully elongate and axis curvature. (D–E) Comparison of craniofacial morphology between a normal larva reared at 0°C (D) and an abnormal larva reared at 4°C (E). Scale bars represent 1 mm and arrows point to a defect in the ventral part of the eye and the fixed open mouth. (F) Quantification of deformities in near-hatch embryos reared at 0°C and at 4C. (G) Total length just before first hatching at 0°C (149 dpf) and at 4°C (86 dpf) (Table S2). *** indicates significance with a Wilcoxon rank sum exact test, p value = 0.008.

common abnormalities involved embryos with kinked, bent, and shortened tails.

Although their rate of growth was faster at 4°C (0.13 mm/day heated, 0.1 mm/day ambient; Figure S6), experimental embryos approaching hatching were shorter (10.98 mm ± 1.47 at 86 dpf (mean ± SD)) than were controls (14.30 mm ± 0.47 at 149 dpf) (Figure 3G, see also Figure 2D′,E). Hatchlings of both treatments had consumed most of their yolk but retained large yolk sacs, as reported previously (Postlethwait et al. 2016; Iken et al. 1997) (Figure 2D′,E; Table S2).

2.4 | Development at Elevated Temperature Altered the Transcriptomic Profiles of Embryos and Hatchlings

To evaluate the effect of elevated temperature on *N. coriiceps* development at the molecular level, we performed bulk RNA sequencing on entire individual embryos collected at the morphological milestones previously described: heartbeat onset (HB), 50% eye pigmentation (EP), eye iridescence (EI), and hatching (H). We aligned sequencing reads to the genome assembly of close relative *Notothenia rossii* (GenBank ID: GCA_949606895.1; Bista et al. 2024) rather than to the *N. coriiceps* genome assembly (GCA_000735185.1; Shin et al. 2014) because of greater contiguity (contig N50: 383.4 kb vs. 17.5 kb) and BUSCO completeness (94.9% vs. 77.3% single copy orthologs) of *N. rossii*'s genome assembly. Differential gene expression (DGE) was analyzed using both DESeq2 and EdgeR, which apply geometric normalization and trimmed mean of M values normalization, respectively (Love et al. 2014; Anders and Huber 2010; Robinson and Oshlack 2010). In total, we estimated DGE for 21,172 genes that passed gene-level filtering criteria out of 24,432 annotated genes. Genes were considered significantly differentially expressed only if they were significant by both methods at FDR-adjusted $p \leq 0.05$. For simplicity, all reported expression values are from the DESeq2 output. Figure S7 shows that sample expression profiles clustered by developmental stage rather than temperature treatment. Stage-specific clustering was not the result of the number of days of development per se (see dpf annotations in Figure S7), indicating that comparable transcriptional profiles for treated and control animals were recovered between stage-matched samples using our morphology-based approach.

We found that hundreds of genes were highly differentially expressed (log2FoldChange > 1 or < −1) at each developmental stage: 1226 at heartbeat onset, 940 at 50% eye pigmentation, 651 at eye iridescence, and 859 at first hatching (Figure 4A, Table S3). The variability of gene expression between the two

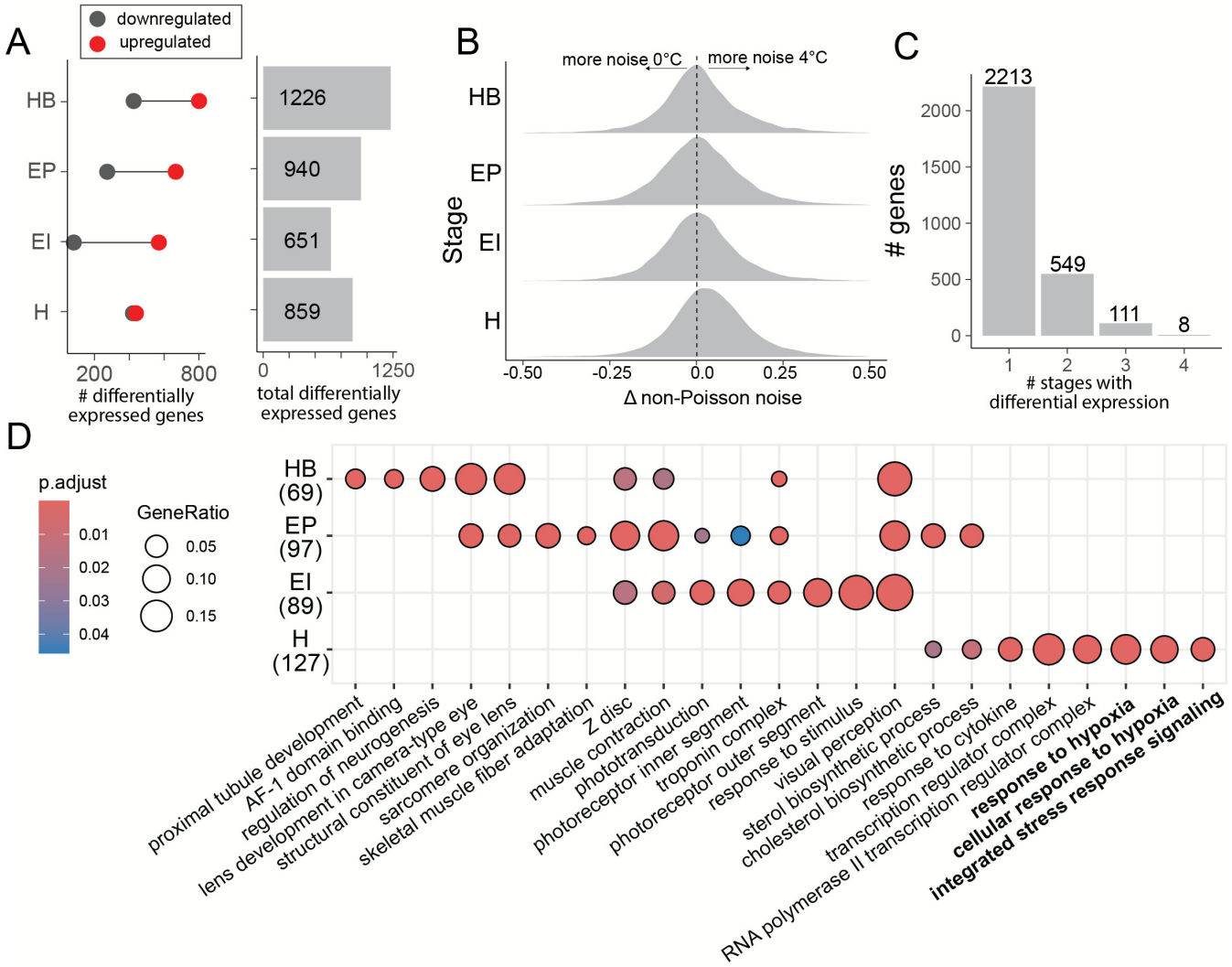

FIGURE 4 | Patterns of differential gene expression during *N. coriiceps* development. (A) Number of genes significantly differentially expressed at each stage (*p*adj ≤0.05, LFC ≤ −1 or ≥1). Red dots indicate genes upregulated at 4°C, gray dots indicate genes downregulated at 4°C relative to 0°C, and gray bars represent the total number of differentially expressed genes at each stage. (B) Distribution of the difference in non-Poisson noise for each gene between treatments (GAMLSS) (Suckling et al. 2015). Positive values indicate greater transcriptional variance at 4°C versus 0°C. (C) Number of genes differentially expressed at one, two, three, or all four developmental stages. (D) Dot plot of Gene Ontology (GO) enrichment over developmental time. The top six enriched GO terms at each stage are shown. Dot size represents the proportion of genes within a GO term that are differentially expressed, while color indicates statistical significance (FDR-adjusted *p*). For (A–D), developmental stages include first heartbeat (HB), 50% eye pigmentation (EP), eye iridescence (EI) and first hatching (H). Numbers in parentheses indicate the total number of significantly enriched terms of the upregulated genes at each stage.

temperature treatments was similar for most of development, but at hatching, more genes showed a qualitative increase in non-Poisson noise at 4°C compared to 0°C (Figure 4B). To our surprise, most differentially expressed genes in at least one of the studied developmental stages (2231 of 2881 genes) were specific to a single developmental stage (Figure 4C). Only 34 genes were differentially expressed at all stages (FDR-adjusted $p \leq 0.05$), eight of which had high expression differences (log2FoldChange ≥1 or ≤−1) (Table S3). Six of these eight were *apolipoprotein B a* (*apoba*), *caveolin 4 a* (*cav4a*), *4-hydroxyphenylpyruvate dioxygenase* (*hpdb*), *insulin-like growth factor binding protein acid labile subunit* (*igfals*), *keratin 4* (*krt4*), and *switching B cell complex subunit 70 a* (*swap70a*). The remaining two genes lacked prior annotation but were identified by BLAST as homologous to *b cell lymphoma 2 like 16* (*bcl2l16*) and *formin-like protein 20* (*LOC104963861*, *N. coriiceps*) (Table S3).

We then investigated whether differentially expressed genes were enriched for specific biological functions using the enricher function in ClusterProfiler v4.14.4 (Yu et al. 2012). Genes upregulated at 4°C showed significant enrichment for 69 gene ontology (GO) terms at heartbeat, 97 at 50% eye pigmentation, 89 at eye iridescence, and 127 at first hatching stages (FDR-adjusted $p \leq 0.05$, Table S4). The GO terms enriched for upregulated genes at HB were related to vision, neurogenesis, and muscle development; at EP to sterol biosynthesis and muscle function; at EI to visual perception, stimulus response, and troponin complex; at H to stress response, hypoxia, and transcription (Figure 4D, Table S4). Genes downregulated at 4°C

were enriched for 16 GO terms at HB, 78 at EP, 10 at EI, and 119 at H (Table S4). The GO terms for downregulated genes at HB were linked to transmembrane transport; at EP to Notch signaling and neurogenesis; at EI to interneuron migration; at H to glucuronidation, steroid metabolism, and hemostasis (Figure 4D, Table S4). Most enriched GO terms were specific to one stage; none occurred across all stages, and hypoxia-related terms appeared only at hatching (Figure 4D, Table S4).

We anticipated that temperature elevated beyond evolved thermal limits would disrupt developmental signaling due to the pleiotropic disruption of most cellular processes (Irvine 2020) and due to the observation of morphological abnormalities (Figure 3). However, we found that only the Notch signaling pathway was consistently enriched (both up- and downregulated) in the GO enrichment analysis and was dysregulated at all stages except EI. Other pathways (Bmp, Fgf, Wnt, Hedgehog) were not enriched for expression dysregulation, although a few individual developmental pathway members were differentially expressed (Tables S3 and S4).

2.5 | Transcriptomes of Thermally Stressed Larvae Exhibited Molecular Signatures of Hypoxia and Cellular Stress

We hypothesized that stress-related genes would be consistently upregulated at +4°C throughout development. Results, however, showed increased transcriptional noise and enrichment for cellular stress responses (e.g., hypoxia, oxidative stress, and mitochondrial dysfunction) in heated embryos only at hatching compared to controls (Figure 4B,D; Table S4). Several highly upregulated genes at hatching are involved in the cellular response to hypoxia, including the key oxygen sensors *egl-9 family hypoxia-inducible factor 2* (*egln2*, also known as *phd1*; see Section 4) and *egl-9 family hypoxia-inducible factor 3* (*egln3*/*phd3*), both of which act upstream of *hypoxia-inducible factor 1-alpha* (*hif1a*) signaling (Figure 5B,C; Table S3) (Ivan and Kaelin Jr 2017). Downstream Hif targets involved in anaerobic metabolism (e.g., *ldha*, *pfkfb3/pfk2*) were also upregulated (Figure 5A–C; Table S3). Upregulation of these glycolytic genes would be expected to enhance anaerobic metabolism under low oxygen conditions (Kierans and Taylor 2021).

The unfolded protein response (UPR) can be activated by hypoxia, which disrupts oxidative protein folding in the endoplasmic reticulum (ER) (Bartoszewska and Collawn 2020). Several core UPR genes were upregulated at hatching at +4°C: *reticulum oxidoreductase 1 alpha* (*ero1a*) and *protein disulfide isomerase family A member 6* (*pdia6*) encode proteins involved in oxidative protein folding. *Eukaryotic translation initiation factor 2 alpha kinase 3* (*eif2ak3*/*perk*) and *activating transcription factor 6* (*atf6*) encode proteins that serve as initial sensors of protein folding stress. *DNA damage-inducible transcript 3* (*ddit3*/*chop*) encodes a transcription factor whose downstream targets include *ero1a* and *tribbles pseudokinase 3* (*trib3*) (Figure 5B,C; Table S3). The *ero1a* and *trib3* genes, which are involved in autophagy and apoptosis in response to protein folding stress (Saleem and Biswas 2017; Hua et al. 2015; Johnson et al. 2020), were two of the most upregulated genes at hatching at +4°C. Finally, *DNA damage-inducible transcript 4* (*ddit4*/*redd1*), a negative regulator of translation that functions downstream of various cellular stress response pathways (Kim et al. 2023), was also upregulated during hatching at +4°C (Figure 5B,C; Table S3). Together, the enrichment data suggest substantial hypoxic and proteostatic cellular stress in heated embryos at hatching but not before hatching.

3 | Discussion

3.1 | Developmental Teratologies in Heated Embryos

Modest warming of the Southern Ocean is likely to disrupt embryonic development of its stenothermal fauna, whether vertebrate or invertebrate. Our findings for *N. coriiceps* align with thermal tolerance studies of several Antarctic invertebrates. Antarctic krill (*Euphausia superba*) embryos show reduced hatching success at 3°C, and 50% of nauplii are abnormal at 5°C (Perry et al. 2020). Normal development of embryos of the Antarctic sea urchin, *Sterechinus neumayeri*, drops significantly with a small increase in temperature (80% normal development at 1°C vs. only 30% at 3°C) at 48 h post-fertilization (hpf) (Bloomer et al. 2023). Similarly, Antarctic starfish (*Odontaster* spp.) embryos reach 20% non-viability at 3°C (Stanwell-Smith and Peck 1998). Thus, slight oceanic warming is very likely to have profound impacts on embryonic development in SO species, with few species showing resilience.

We did not observe increased embryonic lethality at +4°C (Figure S4), probably because we applied the temperature ramp after gastrulation and thus avoided highly temperature-sensitive developmental stages (Dahlke, Lucassen, et al. 2020; Bloomer et al. 2023; Del Rio et al. 2021; Martin et al. 2020; Hamor and Garside 1976). Furthermore, we did not address other environmental stressors, such as increasing ocean acidification from rising pCO_2 or freshening of surface waters from melting ice and increased precipitation (IPCC 2022). Elevated pCO_2 reduces overall thermal tolerance in fish adults and embryos (Flynn et al. 2015; Dahlke et al. 2017; Pimentel et al. 2016; Pimentel et al. 2014), including the Antarctic dragonfish, *G. acuticeps* (Flynn et al. 2015). Thus, mortality and malformation of *N. coriiceps* embryos under the IPCC scenario SSP5-8.5 involving multiple stressors would likely be more severe than we report here for a single manipulated stressor.

We observed a high incidence of body-axis curvature in the +4°C embryo population at hatching (Figure 3), a common defect in fish embryos raised at supraphysiological temperature that has been linked to misfolded protein accumulation in notochordal sheath cells (Dorrity et al. 2023). The observed upregulation of UPR genes (e.g., *ddit3*, *atf6*, *perk*, and *ero1a*) in *N. coriiceps* +4°C hatchlings supports proteostatic stress as an important determinant underlying body-axis curvature (Figure 5), as seen in zebrafish (Dorrity et al. 2023). Increased transcriptional noise in hatchlings at +4°C (Figure 4B) may reflect the diverse teratologies observed in this stage of embryogenesis (Figure 3C) or may be driven by cell-type-specific responses to acute cellular stress near hatching

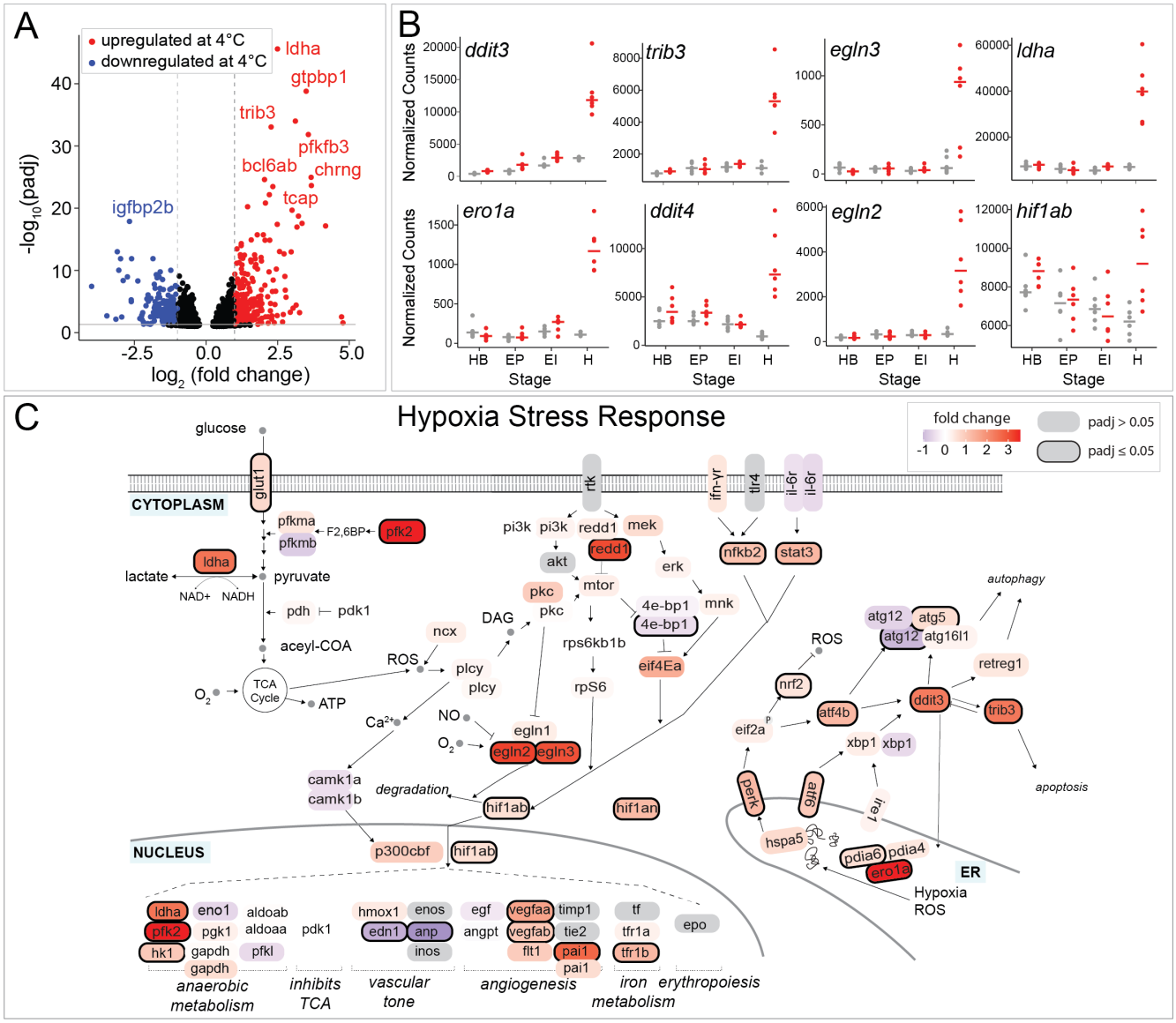

FIGURE 5 | Differential expression of hypoxia and integrated stress response genes during the hatching of *N. coriiceps* embryos. (A) Volcano plot showing differentially expressed genes at hatching. Blue dots represent genes with greater expression at 0°C (padj ≤0.05, LFC ≤1), while red dots denote genes with greater expression at 4°C (*p*adj ≤0.05, LFC ≥1). (B) Expression profiles of selected genes throughout development. Developmental stages include heartbeat (HB), 50% eye pigmentation (EP), eye iridescence (EI) and first hatching (H). Normalized counts are from DESeq2. (C) Diagram of the hypoxia stress response pathway based on KEGG (NT06542, NT06534) (Kanehisa and Goto 2000; Hu et al. 2018; Daskalaki et al. 2018). Each oval is a gene in this pathway, with color indicating $\log_2$ fold change. Genes significantly differentially expressed (*p*adj ≤0.05) are outlined in bold. Genes not identified in the dataset are shown in gray and genes with multiple annotated copies in the *N. rossii* genome are represented twice.

(Dorrity et al. 2023). Body-axis defects, combined with reduced body size, likely would decrease fitness in temperature-stressed embryos, which would impact recruitment success (Miller et al. 1988).

After hatching, embryos transition from relying on yolk reserves to actively feeding, a critical period for survival in fish (Chambers and Trippel 1997). Thus, body size at hatching significantly influences foraging success and starvation resistance (Miller et al. 1988). At +4°C, *N. coriiceps* embryos exhibited reduced growth compared to ~0°C embryos (Figure 3), consistent with a prior study of Atlantic cod subjected to thermal and pH stress (Dahlke et al. 2017). Decreased embryonic growth under stress is thought to reflect the prioritization of essential homeostatic functions over developmental growth (Wieser and Krumschnabel 2001). One stressor, hypoxia, can induce premature hatching in fishes, leading to smaller larvae (Del Rio et al. 2021; Latham and Just 1989; Czerkies et al. 2001; Dimichele and Powers 1984). Our gene expression data for *N. coriiceps* suggests that hypoxia-driven precocious hatching may occur at elevated temperature (Figure 5; see Section 3.4).

3.2 | Timing of Hatching and Phenological Implications

The timing of larval hatching is crucial for survival of zooplankton and for trophic dynamics in planktonic assemblages (Ratnarajah et al. 2023; Beaugrand et al. 2003). Temporal displacements between trophic levels pose challenges to larvae that feed on seasonal prey, thereby impacting fish distributions and food web dynamics (Nielsen et al. 2021; Cooley et al. 2023). Fish embryos possessing large yolk reserves typically have long incubation periods and may be able to delay hatching to align with favorable ecological conditions (Evans et al. 2005; Warkentin 2011; White and Burren 1992; Daniels 1978), though specific hatch-inducing triggers, like hypoxia, may disrupt timing relative to other signals such as light (Fuiman 2009).

Notothenioid embryonic incubation periods range from 1 month in cool-temperate, Sub-Antarctic species like *Patagonotothen tesselata* and *Patagonotothen ramsayi* to 10 months in the high-latitude Antarctic species *Gymnodraco acuticeps* (La Mesa et al. 2021). The developmental time to hatching (~5 months; Figures 1 and 2) that we observed for *N. coriiceps* embryos raised at ambient Palmer Station seawater temperature is consistent with previous reports of 6 months at Palmer Station (Postlethwait et al. 2016), 7 months at King George Island (Sapota 1999), and 5 months at Signy Island (White et al. 1982). *N. coriiceps* embryos hatch with nearly empty yolk sacs (Postlethwait et al. 2016; Iken et al. 1997) (Figure 2D',E), which indicates that they must feed soon after hatching to survive (La Mesa et al. 2021). Because larval abundance of Antarctic fishes correlates with primary productivity (Corso et al. 2022; La Mesa et al. 2010), phenological coupling of hatching with the onset of polar summer is likely crucial for their survival. Our results suggest that hatching of *N. coriiceps* embryos and emergence of feeding larvae at +4°C may become decoupled from the annual daylight cycle and thus likely the availability of phytoplankton prey. However, climate modeling predicts that phytoplankton blooms may also occur earlier under some warming scenarios (Asch et al. 2019), which would potentially reduce the impact of phenological decoupling.

3.3 | Shifting Reproductive Windows in an Antarctic Fish

Because temperature strongly influences developmental rates (Figure 2), projected SO warming may uncouple the evolved synchronization between the timing of breeding seasons and the eventual hatching of larvae at a time of food availability. In our study, *N. coriiceps* embryos began hatching in 155 days at 0°C and in 87 days at +4°C. Limited by these two temperature data points for *N. coriiceps* embryos, we used a linear model to project developmental rates under future climate scenarios along the West Antarctic Peninsula (Figure 6). Though notably, data in cods suggest a negative exponential relationship between temperature and developmental rate, with a near linear increase in rate between −1°C and 4°C that asymptotically approaches what is likely a maximum developmental rate beyond 4°C (Laurel et al. 2018). We assumed that temperatures ≥4°C result in non-viable embryos due to morphological defects or hypoxia and that larvae hatching before or during the polar winter are non-viable due to food scarcity. Under present-day conditions (ERA5; Hersbach et al. 2020), eggs are fertilized in May (austral fall), embryos develop over winter, and larvae hatch in mid-October/November during the austral spring phytoplankton bloom (Figure 6A).

Under all future climate projections (Gidden et al. 2019; IPCC 2022), the window where fertilization could occur shifts compared to current conditions such that embryos avoid high temperatures and hatching during the polar winter (Figure 6B,C). In lower emission scenarios, a slightly warmer thermal profile extends the window of embryo viability by accelerating development, thereby lengthening the breeding season by enabling a hypothetical egg fertilized in the spring to hatch before the onset of the winter period. However, in high-emission scenarios, the temperatures rise too much, resulting in developmental problems. By 2100, winter temperatures should still support *N. coriiceps* embryonic development (Figure 6B,C), such that late breeding shifting into winter could improve embryonic survival by allowing hatching in the spring. However, *N. coriiceps* adults exhibit hibernation-like behavior during winter, including reduced heart rate, metabolism, movement, and growth (Campbell et al. 2008), which could make winter breeding improbable unless hibernation is temperature sensitive. Shifting breeding to spring (November) would lead to embryonic hatching during lethal austral summer conditions that exceed 4°C (Figure 6A, red curve on right). The ability of *N. coriiceps* to adapt to future climate change may be determined by whether there is sufficient genetic variation or phenotypic plasticity in breeding behaviors to overcome hibernation-like activity or if individuals have the ability to regulate or delay the timing of hatching to synchronize with phytoplankton bloom schedules.

While this analysis focused on projected average sea surface temperatures, it is likely that local marine heatwaves will also impact embryo and larval survival. Marine heatwaves are expected to increase in intensity globally over the next century (Frölicher et al. 2018). They affect fish larvae both directly through thermal stress and indirectly through phenological mismatches, leading to dramatic changes in fish assemblages following single heatwave events (Nielsen et al. 2021; Almeida et al. 2024). Recent heatwaves in the West Antarctic Peninsula have reduced primary production and shifted plankton community structure (De Leij et al. 2022). As the composition of phytoplankton communities is highly diverse, more research is required to assess how community structure may impact feeding and recruitment in Antarctic fish larvae (Antoni et al. 2020; Latorre et al. 2023).

3.4 | Hypoxia During Thermal Stress

Our transcriptomic findings align with the hypothesis that hypoxia is a key factor in the thermal sensitivity of *N. coriiceps* embryos (Figures 4 and 5). These results are consistent with the oxygen- and capacity-limited thermal tolerance (OCLTT) concept, which posits that thermal tolerance boundaries are set when temperature-dependent oxygen demand exceeds an organism's aerobic capacity (Pörtner et al. 2017). Warmer temperatures accelerate biochemical reactions, resulting in increased oxygen demand that may not be met by the fixed rate of oxygen

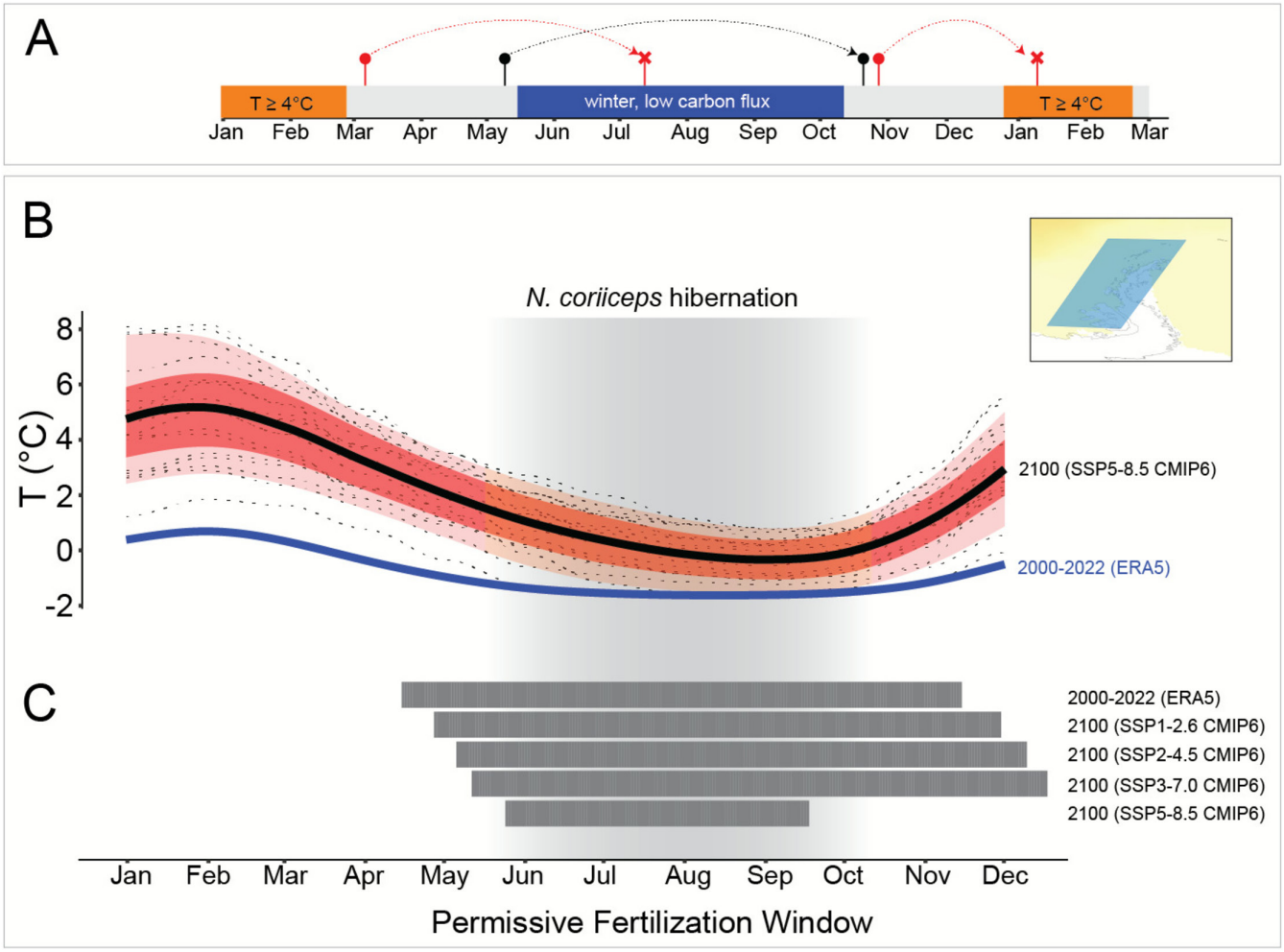

FIGURE 6 | Modeling the timing of fertilization for *N. coriiceps* embryos in a changing climate. (A) Overview of development and hatch timing for *N. coriiceps* embryos. Fertilization is timed so that hatchlings emerge in polar spring. However, complications during development may arise if: (1) temperatures exceed 4°C, or (2) hatching occurs before or during the polar winter (April–October), when food availability is low. Red lines indicate examples of non-viable developmental windows from fertilization to hatching. Black lines indicate an example viable developmental window (B) Plot of monthly SST projections under a high carbon emissions scenario (SSP5-8.5), compared to the average monthly SST from 2000 to 2022 (ERA5). Dashed lines represent different climate models, the dark black line represents the smoothened median, and the red and pink shading indicates the 25–75th and 10–90th percentiles, respectively. (C) Bars represent fertilization dates that meet the criteria outlined in panel (A). Approximate dates of hibernation for adult *N. coriiceps* are shaded in gray in panels (B) and (C) (Campbell et al. 2008).

diffusion across the chorion (Martin et al. 2020; de Salvo Souza et al. 2001; Kranenbarg et al. 2000; Martin et al. 2017; Somero et al. 2016; Schulte 2015). Larger eggs, common in cold climates, further increase hypoxia risk since metabolic rate scales with egg size (La Mesa et al. 2021; Martin et al. 2017; Barneche et al. 2018). As temperatures rise, polar fish embryos are thus likely at an elevated risk for hypoxia.

Embryonic thermal sensitivity shifts throughout development. In teleosts, oxygen consumption peaks at gastrulation and at hatching but is generally lower during mid-development, aligning with periods of highest temperature-induced mortality (Bloomer et al. 2023; Del Rio et al. 2021; Martin et al. 2020; Hamor and Garside 1976; Rombough 2023; Evans et al. 2006). For example, the dragonfish *G. acuticeps* in −1°C to −0.5°C water at McMurdo Sound can briefly tolerate temperatures above 8°C after gastrulation but shows mortality at just 2°C if heating commences during gastrulation (Flynn et al. 2015; Flynn and Todgham 2018). Consistent with these observations, we observed molecular signatures of hypoxia only at hatching and not at earlier developmental stages where oxygen demand is less (Figures 4 and 5).

As described under *Embryo culture* (Section 4), we observed comparable levels of oxygen saturation in the effluent of the ambient (0°C) and elevated (4°C) incubators during the early phases of this experiment, suggesting that dissolved oxygen was not depleted by the embryos (45–56 dpf; Table S5). However, the 4°C water had a lower absolute concentration of oxygen, consistent with reduced solubility of oxygen at higher temperatures (Table S5). We note that these measurements might not reflect conditions within the incubator trays during hatching. Furthermore, embryos experiencing open ocean conditions are unlikely to be as densely packed as those in our experimental apparatus. Nevertheless, the molecular signatures of hypoxia that we observed are specific to embryos of the heated group, consistent with unmet oxygen demand under thermal stress.

3.5 | Adaptability of Antarctic Fishes to Warming

The temperature changes modeled in this study are predicted to occur gradually over multiple generations. In other fish clades, populations and closely related species can differ significantly in embryo thermal tolerance (e.g., Laurel et al. 2018; Blanchard et al. 2024), indicating that thermal tolerance can be an evolvable trait. Notothenioids are characterized by slow generation times, which often exceed 5–15 years, with *N. coriiceps* reaching maturity in about 5–7 years (Calì et al. 2017; La Mesa and Vacchi 2001; Kock 2005). These slow generation times would be predicted to limit their capacity to rapidly adapt to changing climates (Martin et al. 2023; Peck 2005).

We recognize that multiple caveats apply to the interpretation of our results. First, *N. coriiceps* has a wide distribution in the Southern Ocean, ranging as far north as some sub-Antarctic islands (Novillo et al. 2024) (Figure 1B). Populations at the northern limits of this range currently experience temperatures higher than those found along the Antarctic Peninsula (Figure 1B), and they may have greater capacities to acclimatize to future oceanic warming. Second, organismal populations can be sustainable even when small numbers of embryos survive to reproduce (Peck 2023). We found that 35% of near-hatching *N. coriiceps* embryos raised at 4°C lacked conspicuous morphological deformities beyond a shortened length (Figure 3F). Thus, *N. coriiceps* populations may already possess sufficient standing genetic variation in embryonic thermal tolerance to withstand future warming scenarios. Third, this study did not encompass thermal acclimation of parents or transgenerational effects of heating, both of which have been reported to mitigate the impact of stressors such as pH and temperature on developing embryos of ectotherms (Butzge et al. 2021; Rodríguez-Romero et al. 2016; Suckling et al. 2015). Finally, our experiments do not address other evolutionary and ecological factors, including population size, gamete and embryo numbers per spawning, number of spawning events per adult lifetime, dispersal ability, and other factors that can contribute to recruitment and the maintenance of an effective population size (Peck 2011). Nevertheless, our findings argue that peninsular populations of *N. coriiceps* are at risk for developmental abnormalities and reduced larval recruitment as their habitat warms, with important implications for ecosystem structure and function.

Several notothenioid lineages originally from Antarctic waters have successfully adapted to warmer conditions north of the polar front (Eastman 2005; Papetti et al. 2016). One example is the Maori chief/black cod (*Paranotothenia angustata*), a close relative of *N. coriiceps*, which inhabits warmer coastal waters around New Zealand and Australia. Compared to *N. coriiceps*, *P. angustata* has secondarily evolved higher thermal tolerance in adults (Bilyk and Devries 2012). Little is currently known about *P. angustata* reproduction and embryogenesis. Compared to results presented here, studying how these temperate-adapted notothenioids cope with warming as embryos would help to project the responses of Antarctic fishes to climate change and to identify developmental genetic mechanisms driving the evolution of thermal tolerance.

3.6 | Summary

Our data revealed that projected temperature increases [4°C, by 2100–2200, unmitigated climate emission scenario Shared Socioeconomic Pathways (SSP5-8.5) (IPCC 2022; Swart et al. 2019)] over the next 100–200 years are likely to severely impact *N. coriiceps* embryo development, causing high rates of morphological abnormalities, molecular stress responses, and asynchrony between developmental rates and seasonal environmental conditions. Although a +4°C sea surface temperature increase is currently on the extreme end of climate projections, transient seasonal variability or marine heatwaves from a higher baseline temperature could disrupt reproduction in *N. coriiceps* and other Antarctic fish. Similar studies across the life cycle of other organisms with diverse egg and embryo characteristics may provide key data points needed to improve the accuracy of predictive climate change models.

4 | Materials and Methods

4.1 | Fish Collection, Maintenance, and Spawning

Adult *N. coriiceps* specimens were collected south of Low Island and west of Brabant Island (Dallman Bay) along the West Antarctic Peninsula between April 20 and May 28 of 2018 (Figure 1C). Eighty specimens were captured by deploying Otter trawls and baited traps from the *ARSV Laurence M. Gould* as previously described (Desvignes et al. 2019). Fish were maintained onboard ship in six 1 m^3 flow-through isothermic tanks (Xactics, Cornwall, Ontario, Canada) with supplemental aeration. The fish were transferred within 2 days to the Palmer Station aquatic laboratories, where they were held in 2.5-m^3 circular tanks supplied with flow-through, filtered, and aerated seawater from Arthur Harbor, as previously described (Le François et al. 2017). Sexually mature adults were housed at an average of 25 fish per tank.

To promote gonadal maturation in captivity, males and females received up to two intraperitoneal injections of salmon gonadotropin-releasing hormone (GnRH) analog as an ovulating and spermiating agent at a dosage of 0.5 mL/kg (Ovaprim Syndel, Ferndale, WA, USA). Tanks were checked several times a day for signs of spontaneous broadcast spawning, such as floating eggs or large amounts of foam on the surface due to tank aeration interacting with protein in the water. In total, there were 14 spawning events over 12 days. The first four spawning events were pooled to create the group of embryos used in this experiment, with 0 days post-fertilization (dpf) designated as the date most eggs were fertilized (two spawns on 5/26/2018 versus one each on 5/25/2018 and 5/27/2018). Spawning most likely involved mixed parentage as multiple males and females could have released gametes. All procedures were performed in accordance with the Animal Care and Use Committee (IACUC) at Northeastern University (#15-0207R).

4.2 | Embryo Culture

Embryos were cultured in two flow-through vertical incubation systems operated at Palmer Station (Marisource, WA, USA) in a walk-in refrigerated room kept at 2°C (Figure S1). Seawater

pumped directly from Arthur Harbor was first sand-filtered, then sterilized with UV light, and dispatched into two 50-L LLDPE reservoir tanks (Nalgene, Thermo Fisher Scientific, USA). Water in the reservoir tanks was oxygenated with air pumps before being distributed into the top section of the incubation systems (Figure S1). Due to fieldsite constraints, we were unable to set up independent culture systems that were fed by separate ambient and heated head tanks. One of the two reservoir tanks was heated to 4°C ± 0.2°C using three feedback-controlled submersible heaters, while the other one was kept at ambient temperature. Oxygen levels were measured at the bottom of both incubator towers 45–56 dpf using a handheld multiparameter meter (Pro2030 Dissolved Oxygen/Conductivity Meter (YSI Inc. Yellowspring, OH, USA)); they remained relatively stable (102.08% ± 0.72% saturation at 0°C and 100.88% ± 0.53% saturation at 4°C) across incubator drawers (Table S5).

Fertilized *N. coriiceps* eggs averaged 4.36 ± 0.03 mm in diameter and 0.05 ± 0.002 g in wet weight. A total of 2.19 kg (~44,000 embryos) were used, with 482 g placed in two incubator drawers at 0°C. At 15 days post-fertilization (dpf), 241 g of embryos per tray were transferred to an aerated incubator separate from the main incubation trays, then gradually heated by 1°C a day until reaching +4°C 4 days later at 19 dpf. Heated embryos were then moved to the heated vertical incubator system. Temperatures in both incubator systems were taken once an hour and averaged for each day using immersed temperature loggers inserted in the incubator trays (Alphamach, DS1922L) (Figure S3). Average temperatures were 0.21°C ± 0.28°C (ambient, 1 dpf to 142 dpf) and 4.10°C ± 0.48°C (heated, 19 dpf to 100 dpf). A sensor malfunction temporarily stopped heating in the heated reservoir tank, dropping the temperature of the heated incubator trays toward ambient water temperatures. This resulted in the heated incubator reaching 1°C at 83 dpf. This incubator was ramped back up to 4°C by 87 dpf.

Embryos were disinfected biweekly with an immersion in 400 ppm glutaraldehyde water bath in filtered, UV-sterilized seawater for 10 min to control potential microbial growth. Dead embryos were removed prior to disinfection and mortality was evaluated by changes in wet weight or by counting individual dead embryos, depending on the volume of dead embryos. Every 7 days, five embryos were randomly sampled and photographed under a dissecting microscope, and their lengths were measured using an open-source image analysis software platform (ImageJ; Schneider et al. 2012) with scale bars calibrated to the scope camera.

4.3 | RNA Extraction and Sequencing

To account for different developmental rates at 0°C and 4°C, samples were collected at fixed ages of 30, 60, 90, and 120 days post-fertilization (dpf) and at key developmental milestones heartbeat (HB), 50% eye pigmentation (EP), eye iridescence (EI), and hatching (H). These stages were selected for their clear visibility under a dissecting scope and relatively even distribution throughout development. 120 embryos per time point (30 per technical replicate per treatment) were randomly collected, with chorions pierced for fixative penetration. Whole embryos were preserved in groups of 30 per tube in RNAlater (#AM7201; Invitrogen, Waltham, MA, USA). These tubes of embryos were placed at 4°C for 24 h, at which point they were moved to −80°C for long-term storage. Genomic DNA and total RNA were extracted from single embryos using the Zymo Quick DNA/RNA Kit (#D7001; Zymo, Irvine, CA, USA). Due to their large size (~12 mm TL), hatchlings were first digested with 20 mg/mL proteinase K solution during a 1 h incubation at room temperature in lysis buffer to ensure full cell dissociation and rupture. RNA extract quality was assessed using an Agilent Tapestation, and only samples with a RNA Integrity Number (RIN) > 6.4 were further processed. Stranded Illumina sequencing libraries were prepared from six replicates per treatment and time point (48 total libraries) at the University of Oregon's Genomics and Cell Characterization Core Facility (GC3F) using the NuGen Universal Plus mRNA Kit (#0520-A01, Tecan Life Sciences, Männedorf, Switzerland). Resulting libraries were sequenced with paired-end 150 bp reads on an Illumina NovaSeq 6000, averaging 47.3 ± 6.1 million reads per sample (Table S6).

4.4 | RNA Differential Expression and Variance Analysis

The quality of sequenced libraries was visualized using FastQC 0.11.9, where adapter content was seen in some samples. Therefore, adapter trimming was performed with Cutadapt v1.18 ("--nextseq-trim=18 --minimum-length 20") to remove universal Illumina adaptors (Martin 2011). Trimmed sequences were aligned to the *Notothenia rossii* genome assembly (GCA_949606895.1; Bista et al. 2024) using HiSat2 v2.2.1 with relaxed mismatch and gap penalties to accommodate polymorphisms between *N. coriiceps* reads and the *N. rossii* genome sequence (parameters "--mp 4,1 --rdg 4,2 --rna-strandness FR --dta") (Kim et al. 2019; Kim et al. 2015). On average, 85.5% ± 1.3% of *N. coriiceps* reads aligned to the *N. rossii* assembly (Table S6). Transcript annotation of the *N. rossii* assembly derived from the Ensembl Genebuild annotation system (Aken et al. 2016). Transcript-level expression was estimated with StringTie v1.3.3 (Pertea et al. 2015) and summarized at the gene level using tximport v1.34.0 (Soneson et al. 2015). Differential expression analysis was conducted with DESeq2 v1.46.0 and EdgeR v4.4.1 (Anders and Huber 2010; Robinson and Oshlack 2010). Genes were considered differentially expressed only if they were statistically significant with both tools. Fold change and p values are reported from DESeq2, with p values adjusted for multiple testing (FDR). Non-Poisson noise in read count data was estimated using GAMLSS (ExpVarQuant; De Jong et al. 2019), and the difference in non-Poisson noise between +4°C and 0°C was calculated for each gene. Gene names not found in *N. rossii* annotations were assigned by identifying orthologs in the genome of the channel bull blenny (*Cottoperca trigloides*, GCA_900634415.1; Bista et al. 2020) using BLAST+ v2.14.1 (Camacho et al. 2009).

4.5 | Gene Ontology Enrichment

Since *N. rossii* and *N. coriiceps* lack Gene Ontology (GO) annotations, we used data from the orthologous genes of other vertebrate species. We used OrthoFinder v2.2.6 (Emms and Kelly 2019) to identify one-to-one orthologs between *N. rossii* and *C. trigloides*. Genes without orthologs or with many-to-many matches were

excluded. GO data were retrieved from *C. trigloides* and Ensembl BioMart-predicted orthologs in human, mouse, chicken, and zebrafish (accessed March 2023) (Kinsella et al. 2011). Ensembl gene IDs were then converted into a final, non-redundant *C. trigloides* ortholog set. Functional pathway enrichment was analyzed using clusterProfiler v4.14.4 (Yu et al. 2012; Wu et al. 2021). Certain gene names had more recognizable common names relevant to other taxa. Multiple designations were included for these genes to capture audiences that recognize these genes by different names, rather than only fish-related genes.

4.6 | Modeling Development Windows Under Future Climate Scenarios

We predicted embryonic viability based on two assumptions supported by the current data: (1) development must occur at ≤4°C to complete without abnormalities or hypoxia, and (2) hatching between April and October would increase starvation risk due to limited primary productivity, which is correlated with larval abundance (Figure 6A) (Corso et al. 2022; La Mesa et al. 2010; Daly 2004; Bernard et al. 2022). To assess future conditions, we used the Coupled Model Intercomparison Project Phase 6 (CMIP6) median sea surface temperature projections for 2100 from the Copernicus Interactive Climate Atlas (Figure 6B,C) and ERA5 data for current conditions (2000–2022) (Figure 6B,C) (Swart et al. 2019; Hersbach et al. 2020).

For each possible fertilization date in the year, we estimated hatching timing and checked for non-permissive developmental temperatures and hatching outside the food resource window. Development duration was assessed using a linear model constrained by known values: 3672 h (153 days) at 0°C and 2088 h (87 days) at +4°C. The function interpolates the development rate between these points using a linear relationship, expressed as:

$$r(T) = \frac{1}{3672 - \left(T \times \frac{3672 - 2088}{4}\right)} \text{ for } -1^{\circ}\text{C} \le T \le 5^{\circ}\text{C} \quad (1)$$

where $r(T)$ represents the fraction of development completed per hour at a given temperature (T). The developmental rate, $r(T)$, was interpolated between −1°C and 5°C to ensure realistic projections. Most current and projected temperatures fall within this range, with modern ERA5 temperatures between −1.62°C and 0.69°C and median of future climate models (SSP5-8.5) between −0.38°C and 5.10°C.

To refine temperature data, we interpolated monthly median temperatures from climate models using a cubic spline method, increasing resolution to an hourly scale. Developmental progress was then computed via numerical integration using the trapezoidal rule with the python function scipy.integrate.cumulative_trapezoid, which approximates the integral as:

$$D_n = \sum_{k=1}^{n} \frac{1}{2}\left(r(T_k) + r(T_{k-1})\right) \times \Delta k$$

where $D(n)$ is the cumulative fraction of development completed at time n. Hatch timing is calculated by locating the time at which D reaches 1 (i.e., full development). If temperatures exceeded 4°C during development or hatching occurred between April and October, the fertilization date was considered unsuitable.

Author Contributions

M.S., N.R.L.F., T.D., J.H.P., H.W.D., and J.M.D. designed research; M.S., N.R.L.F., T.D., J.G., J.H.P., and J.M.D. performed research; M.S., H.W.D., and J.M.D. analyzed data; and M.S. and J.M.D. wrote the paper; M.S., N.R.L.F., T.D., J.G., J.H.P., H.W.D., and J.M.D. provided critical revision of the manuscript.

Acknowledgments

We gratefully acknowledge the support of our research by the captain and crew of the *ASRV Laurence M Gould*, the staff of Palmer Station, the personnel of the Office of Polar Programs of the National Science Foundation, and the staff of the Antarctic Support Contractor (Denver, CO). We also offer our heartfelt thanks to Laura Goetz, Urjeet Khanwalkar, Kathleen Shusdock, Sierra Smith, and Eileen Spann, whose previous work in 2014 and 2016 field seasons laid the foundation for the success of this study. This work was supported by the NSF grants PLR-1444167 (H.W.D.), PLR-2324998 (J.M.D. and H.W.D.), OPP-1543383 (J.H.P., T.D., and H.W.D.), and OPP-2232891 (J.H.P. and T.D.). This work was completed in part with resources provided by the Research Computing Data Core at the University of Houston.

Conflicts of Interest

The authors declare no conflicts of interest.

Data Availability Statement

The data that support the findings of this study are openly available in SRA at https://www.ncbi.nlm.nih.gov/bioproject/PRJNA1289157, BioProject reference number PRJNA1289157.

References

Aken, B. L., S. Ayling, D. Barrell, et al. 2016. "The Ensembl Gene Annotation System." *Database: The Journal of Biological Databases and Curation* 2016: baw093.

Almeida, L. Z., B. Laurel, H. L. Thalmann, and J. A. Miller. 2024. "Warmer, Earlier, Faster: Cumulative Effects of Gulf of Alaska Heatwaves on the Early Life History of Pacific Cod." *Elementa: Science of the Anthropocene* 12: 00050.

Anders, S., and W. Huber. 2010. "Differential Expression Analysis for Sequence Count Data." *Genome Biology* 11: R106.

Antoni, J. S., G. O. Almandoz, M. E. Ferrario, et al. 2020. "Response of a Natural Antarctic Phytoplankton Assemblage to Changes in Temperature and Salinity." *Journal of Experimental Marine Biology and Ecology* 532: 151444.

Asch, R. G., C. A. Stock, and J. L. Sarmiento. 2019. "Climate Change Impacts on Mismatches Between Phytoplankton Blooms and Fish Spawning Phenology." *Global Change Biology* 25: 2544–2559.

Barneche, D. R., S. C. Burgess, and D. J. Marshall. 2018. "Global Environmental Drivers of Marine Fish Egg Size." *Global Ecology and Biogeography* 27: 890–898.

Barrera-Oro, E. R., E. R. Marschoff, and R. J. Casaux. 2000. "Trends in Relative Abundance of Fjord *Notothenia rossii*, *Gobionotothen gibberifrons* and *Notothenia coriiceps* at Potter Cove, South Shetland Islands, After Commercial Fishing in the Area." *CCAMLR Science Journal of the Scientific Committee and the Commission for the Conservation of Antarctic Marine Living Resources* 7: 43–52.

Bartoszewska, S., and J. F. Collawn. 2020. "Unfolded Protein Response (UPR) Integrated Signaling Networks Determine Cell Fate During Hypoxia." *Cellular & Molecular Biology Letters* 25: 18.

Beaugrand, G., K. M. Brander, J. Alistair Lindley, S. Souissi, and P. C. Reid. 2003. "Plankton Effect on Cod Recruitment in the North Sea." *Nature* 426: 661–664.

Beers, J. M., and N. Jayasundara. 2015. "Antarctic Notothenioid Fish: What Are the Future Consequences of "Losses" and "Gains" Acquired During Long-Term Evolution at Cold and Stable Temperatures?" *Journal of Experimental Biology* 218: 1834–1845.

Bernard, K. S., K. B. Steinke, and J. M. Fontana. 2022. "Winter Condition, Physiology, and Growth Potential of Juvenile Antarctic Krill." *Frontiers in Marine Science* 9: 990853.

Bilyk, K. T., and A. L. Devries. 2011. "Heat Tolerance and Its Plasticity in Antarctic Fishes." *Comparative Biochemistry and Physiology. Part A, Molecular & Integrative Physiology* 158: 382–390.

Bilyk, K. T., and A. L. Devries. 2012. "Heat Tolerance of the Secondarily Temperate Antarctic Notothenioid, *Notothenia angustata*." *Antarctic Science* 24: 165–172.

Bilyk, K. T., L. Vargas-Chacoff, and C.-H. C. Cheng. 2018. "Evolution in Chronic Cold: Varied Loss of Cellular Response to Heat in Antarctic Notothenioid Fish." *BMC Evolutionary Biology* 18: 143.

Bista, I., M. Collins, Wellcome Sanger Institute Tree of Life Management, Samples and Laboratory Team, Wellcome Sanger Institute Scientific Operations: Sequencing Operations, Wellcome Sanger Institute Tree of Life Core Informatics Team, and Tree of Life Core Informatics Collective. 2024. "The Genome Sequence of the Marbled Rockcod, *Notothenia rossii* Richardson, 1844." *Wellcome Open Research* 9: 227.

Bista, I., S. A. McCarthy, J. Wood, et al. 2020. "The Genome Sequence of the Channel Bull Blenny, *Cottoperca gobio* (Günther, 1861)." *Wellcome Open Research* 5: 148.

Bista, I., J. M. D. Wood, T. Desvignes, et al. 2023. "Genomics of Cold Adaptations in the Antarctic Notothenioid Fish Radiation." *Nature Communications* 14: 3412.

Blanchard, T. S., M. L. Earhart, A. K. Shatsky, and P. M. Schulte. 2024. "Intraspecific Variation in Thermal Performance Curves for Early Development in *Fundulus heteroclitus*." *Journal of Experimental Zoology Part A: Ecological and Integrative Physiology* 341: 827–844.

Bloomer, J., J. J. Anderson, D. Sear, S. Greene, D. Gantner, and C. Hanson. 2023. "Gastrulation and Hatch as Critical Thermal Windows for Salmonid Embryo Development." *River Research and Applications* 39: 46–53.

Butzge, A. J., T. T. Yoshinaga, O. D. M. Acosta, et al. 2021. "Early Warming Stress on Rainbow Trout Juveniles Impairs Male Reproduction but Contrastingly Elicits Intergenerational Thermotolerance." *Scientific Reports* 11: 17053.

Calì, F., E. Riginella, M. La Mesa, and C. Mazzoldi. 2017. "Life History Traits of *Notothenia rossii* and *N. coriiceps* Along the Southern Scotia Arc." *Polar Biology* 40: 1409–1423.

Camacho, C., G. Coulouris, V. Avagyan, et al. 2009. "BLAST+: Architecture and Applications." *BMC Bioinformatics* 10: 421.

Campbell, H. A., K. P. P. Fraser, C. M. Bishop, L. S. Peck, and S. Egginton. 2008. "Hibernation in an Antarctic Fish: On Ice for Winter." *PLoS One* 3: e1743.

Chambers, R. C., and E. A. Trippel. 1997. "Relationships Between Early Life History Traits and Recruitment Among Coral Reef Fishes." In *Early Life History and Recruitment in Fish Populations*, edited by R. C. Chambers and E. A. Trippel, 423–449. Springer.

Cooley, S. R., D. S. Schoeman, L. Bopp, et al. 2023. "Oceans and Coastal Ecosystems and Their Services." In *Climate Change 2022: Impacts, Adaptation and Vulnerability*, edited by H. O. Pörtner, D. C. Roberts, M. Tignor, et al., 379–550. Cambridge University Press.

Corso, A. D., D. K. Steinberg, S. E. Stammerjohn, and E. J. Hilton. 2022. "Climate Drives Long-Term Change in Antarctic Silverfish Along the Western Antarctic Peninsula." *Communications Biology* 5: 104.

Czerkies, P., P. Brzuzan, K. Kordalski, and M. Luczynski. 2001. "Critical Partial Pressures of Oxygen Causing Precocious Hatching in *Coregonus lavaretus* and *C. albula* Embryos." *Aquaculture* 196: 151–158.

Daane, J. M., and H. W. Detrich. 2022. "Adaptations and Diversity of Antarctic Fishes: A Genomic Perspective." *Annual Review of Animal Biosciences* 10: 39–62.

Dahlke, F., M. Lucassen, U. Bickmeyer, et al. 2020. "Fish Embryo Vulnerability to Combined Acidification and Warming Coincides With a Low Capacity for Homeostatic Regulation." *Journal of Experimental Biology* 223: jeb212589.

Dahlke, F. T., E. Leo, F. C. Mark, et al. 2017. "Effects of Ocean Acidification Increase Embryonic Sensitivity to Thermal Extremes in Atlantic Cod, *Gadus morhua*." *Global Change Biology* 23: 1499–1510.

Dahlke, F. T., S. Wohlrab, M. Butzin, and H.-O. Pörtner. 2020. "Thermal Bottlenecks in the Life Cycle Define Climate Vulnerability of Fish." *Science* 369: 65–70.

Daly, K. L. 2004. "Overwintering Growth and Development of Larval *Euphausia superba*: An Interannual Comparison Under Varying Environmental Conditions West of the Antarctic Peninsula." *Deep Sea Research Part II: Topical Studies in Oceanography* 51: 2139–2168.

Daniels, R. A. 1978. "Nesting Behaviour of *Harpagifer bispinis* in Arthur Harbour, Antarctic Peninsula." *Journal of Fish Biology* 12: 465–474.

Daskalaki, I., I. Gkikas, and N. Tavernarakis. 2018. "Hypoxia and Selective Autophagy in Cancer Development and Therapy." *Frontiers in Cell and Developmental Biology* 6: 104.

De Jong, T. V., Y. M. Moshkin, and V. Guryev. 2019. "Gene Expression Variability: The Other Dimension in Transcriptome Analysis." *Physiological Genomics* 51: 145–158.

De Leij, R., L. J. Grange, and L. S. Peck. 2022. "Functional Thermal Limits Are Determined by Rate of Warming During Simulated Marine Heatwaves." *Marine Ecology Progress Series* 685: 183–196.

de Salvo Souza, R. H., R. Soncini, M. L. Glass, J. R. Sanches, and F. T. Rantin. 2001. "Ventilation, Gill Perfusion and Blood Gases in Dourado, *Salminus maxillosus* Valenciennes (Teleostei, Characidae), Exposed to Graded Hypoxia." *Journal of Comparative Physiology B: Biochemical, Systemic, and Environmental Physiology* 171: 483–489.

Del Rio, A. M., G. N. Mukai, B. T. Martin, et al. 2021. "Differential Sensitivity to Warming and Hypoxia During Development and Long-Term Effects of Developmental Exposure in Early Life Stage Chinook Salmon." *Conservation Physiology* 9: coab054.

Desvignes, T., N. R. le François, L. C. Goetz, et al. 2019. "Intergeneric Hybrids Inform Reproductive Isolating Barriers in the Antarctic Icefish Radiation." *Scientific Reports* 9: 5989.

Devries, A. L. 2020. "Fish Antifreeze Proteins." In *Antifreeze Proteins Volume 1: Environment, Systematics and Evolution*, 85–129. Springer.

Dimichele, L., and D. Powers. 1984. "Developmental and Oxygen Consumption Rate Differences Between Lactate Dehydrogenase-B Genotypes of *Fundulus heteroclitus* and Their Effect on Hatching Time." *Physiological Zoology* 57: 52–56.

Dorrity, M. W., L. M. Saunders, M. Duran, et al. 2023. "Proteostasis Governs Differential Temperature Sensitivity Across Embryonic Cell Types." *Cell* 186: 5015–5027.e12.

Ducklow, H., and P. S. A. Lter. 2014. "Vertical Fluxes of Particulate Carbon, Nitrogen and Phosphorus From a Sediment Trap Deployed

West of Palmer Station, Antarctica at a Depth of 170 Meters, 1992–Present."

Eastman, J. T. 2005. "The Nature of the Diversity of Antarctic Fishes." *Polar Biology* 28: 93–107.

Eastman, J. T., and R. R. Eakin. 2021. "Checklist of the Species of Notothenioid Fishes." *Antarctic Science* 33: 1–8.

Eayrs, C., X. Li, M. N. Raphael, and D. M. Holland. 2021. "Rapid Decline in Antarctic Sea Ice in Recent Years Hints at Future Change." *Nature Geoscience* 14: 460–464.

Egginton, S., M. Axelsson, E. L. Crockett, K. M. O'Brien, and A. P. Farrell. 2019. "Maximum Cardiac Performance of Antarctic Fishes That Lack Haemoglobin and Myoglobin: Exploring the Effect of Warming on Nature's Natural Knockouts." *Conservation Physiology* 7: coz049.

Emms, D. M., and S. Kelly. 2019. "OrthoFinder: Phylogenetic Orthology Inference for Comparative Genomics." *Genome Biology* 20: 238.

Evans, C. W., P. Cziko, C.-H. C. Cheng, and A. L. Devries. 2005. "Spawning Behaviour and Early Development in the Naked Dragonfish *Gymnodraco acuticeps*." *Antarctic Science* 17: 319–327.

Evans, C. W., L. Pace, P. A. Cziko, A. G. Marsh, C. H. C. Cheng, and A. L. DeVries. 2006. "Metabolic Energy Utilization During Development of Antarctic Naked Dragonfish (*Gymnodraco acuticeps*)." *Polar Biology* 29: 519–525.

Flynn, E. E., B. E. Bjelde, N. A. Miller, and A. E. Todgham. 2015. "Ocean Acidification Exerts Negative Effects During Warming Conditions in a Developing Antarctic Fish." *Conservation Physiology* 3: cov033.

Flynn, E. E., and A. E. Todgham. 2018. "Thermal Windows and Metabolic Performance Curves in a Developing Antarctic Fish." *Journal of Comparative Physiology. B* 188: 271–282.

Frölicher, T. L., E. M. Fischer, and N. Gruber. 2018. "Marine Heatwaves Under Global Warming." *Nature* 560: 360–364.

Fuiman, L. A. 2009. "Special Considerations of Fish Eggs and Larvae." In *Fishery Science: The Unique Contributions of Early Life Stages*, edited by F. L. A. R. G. Werner, 1–32. Wiley-Blackwell.

Gidden, M. J., K. Riahi, S. J. Smith, et al. 2019. "Global Emissions Pathways Under Different Socioeconomic Scenarios for Use in CMIP6: A Dataset of Harmonized Emissions Trajectories Through the End of the Century." *Geoscientific Model Development* 12: 1443–1475.

Gon, O., and P. C. Heemstra, eds. 1990. *Fishes of the Southern Ocean*. J.L.B. Smith Institute of Ichthyology.

Hamor, T., and E. T. Garside. 1976. "Developmental Rates of Embryos of Atlantic Salmon, *Salmo salar* L., in Response to Various Levels of Temperature, Dissolved Oxygen, and Water Exchange." *Canadian Journal of Zoology* 54: 1912–1917.

Hersbach, H., B. Bell, P. Berrisford, et al. 2020. "The ERA5 Global Reanalysis." *Quarterly Journal of the Royal Meteorological Society* 146: 1999–2049.

Hobbs, W., P. Spence, A. Meyer, et al. 2024. "Observational Evidence for a Regime Shift in Summer Antarctic Sea Ice." *Journal of Climate* 37: 2263–2275.

Hu, H., M. Tian, C. Ding, and S. Yu. 2018. "The C/EBP Homologous Protein (CHOP) Transcription Factor Functions in Endoplasmic Reticulum Stress-Induced Apoptosis and Microbial Infection." *Frontiers in Immunology* 9: 3083.

Hua, F., K. Li, J.-J. Yu, and Z.-W. Hu. 2015. "The TRIB3-SQSTM1 Interaction Mediates Metabolic Stress-Promoted Tumorigenesis and Progression via Suppressing Autophagic and Proteasomal Degradation." *Autophagy* 11: 1929–1931.

Iken, K., E. R. Barrera-Oro, M. L. Quartino, R. J. Casaux, and T. Brey. 1997. "Grazing by the Antarctic Fish *Notothenia Coriiceps*: Evidence for Selective Feeding on Macroalgae." *Antarctic Science* 9: 386–391.

Intergovernmental Panel on Climate Change (IPCC). 2022. *The Ocean and Cryosphere in a Changing Climate: Special Report of the Intergovernmental Panel on Climate Change*. Cambridge University Press.

Irvine, S. Q. 2020. "Embryonic Canalization and Its Limits—A View From Temperature." *Journal of Experimental Zoology. Part B, Molecular and Developmental Evolution* 334: 128–144.

Iturbide, M., J. Fernández, J. M. Gutiérrez, et al. 2022. "Implementation of FAIR Principles in the IPCC: The WGI AR6 Atlas Repository." *Scientific Data* 9: 629.

Ivan, M., and W. G. Kaelin Jr. 2017. "The EGLN-HIF O2-Sensing System: Multiple Inputs and Feedbacks." *Molecular Cell* 66: 772–779.

Johnson, B. D., W. J. Geldenhuys, and L. A. Hazlehurst. 2020. "The Role of ERO1α in Modulating Cancer Progression and Immune Escape." *Journal of Cancer Immunology* 2: 103–115.

Kamler, E. 2012. *Early Life History of Fish: An Energetics Approach*. Springer.

Kanehisa, M., and S. Goto. 2000. "KEGG: Kyoto Encyclopedia of Genes and Genomes." *Nucleic Acids Research* 28: 27–30.

Kellermann, A. 1991. "EGG and Larval Drift of the Antarctic Fish Notothenia Corriceps." *Cybium* 15: 199–210.

Kierans, S. J., and C. T. Taylor. 2021. "Regulation of Glycolysis by the Hypoxia-Inducible Factor (HIF): Implications for Cellular Physiology." *Journal of Physiology* 599: 23–37.

Kim, D., B. Langmead, and S. L. Salzberg. 2015. "HISAT: A Fast Spliced Aligner With Low Memory Requirements." *Nature Methods* 12: 357–360.

Kim, D., J. M. Paggi, C. Park, C. Bennett, and S. L. Salzberg. 2019. "Graph-Based Genome Alignment and Genotyping With HISAT2 and HISAT-Genotype." *Nature Biotechnology* 37: 907–915.

Kim, J.-Y., Y.-G. Kwon, and Y.-M. Kim. 2023. "The Stress-Responsive Protein REDD1 and Its Pathophysiological Functions." *Experimental & Molecular Medicine* 55: 1933–1944.

Kinsella, R. J., A. Kähäri, S. Haider, et al. 2011. "Ensembl BioMarts: A Hub for Data Retrieval Across Taxonomic Space." *Database* 2011: bar030.

Kock, K.-H. 2005. "Antarctic Icefishes (Channichthyidae): A Unique Family of Fishes. A Review, Part I." *Polar Biology* 28: 862–895.

Kranenbarg, S., M. Muller, J. L. Gielen, and J. H. Verhagen. 2000. "Physical Constraints on Body Size in Teleost Embryos." *Journal of Theoretical Biology* 204: 113–133.

La Mesa, M., B. Catalano, A. Russo, S. Greco, M. Vacchi, and M. Azzali. 2010. "Influence of Environmental Conditions on Spatial Distribution and Abundance of Early Life Stages of Antarctic Silverfish, *Pleuragramma antarcticum* (Nototheniidae), in the Ross Sea." *Antarctic Science* 22: 243–254.

La Mesa, M., F. Llompart, E. Riginella, and J. T. Eastman. 2021. "Parental Care and Reproductive Strategies in Notothenioid Fishes." *Fish and Fisheries* 22: 356–376.

La Mesa, M., and M. Vacchi. 2001. "Age and Growth of High Antarctic Notothenioid Fish." *Antarctic Science* 13: 227–235.

Latham, K. E., and J. J. Just. 1989. "Oxygen Availability Provides a Signal for Hatching in the Rainbow Trout (*Salmo gairdneri*) Embryo." *Canadian Journal of Fisheries and Aquatic Sciences* 46: 55–58.

Latorre, M. P., C. M. Iachetti, I. R. Schloss, et al. 2023. "Summer Heatwaves Affect Coastal Antarctic Plankton Metabolism and Community Structure." *Journal of Experimental Marine Biology and Ecology* 567: 151926.

Laurel, B. J., L. A. Copeman, M. Spencer, and P. Iseri. 2018. "Comparative Effects of Temperature on Rates of Development and Survival of Eggs and Yolk-Sac Larvae of Arctic Cod (*Boreogadus saida*) and Walleye Pollock (*Gadus chalcogrammus*)." *ICES Journal of Marine Science* 75: 2403–2412.

Le François, N. R., E. Sheehan, T. Desvignes, C. Belzile, J. H. Postlethwait, and H. W. Detrich III. 2017. "Characterization and Husbandry of Wild Broodstock of the Blackfin Icefish *Chaenocephalus aceratus* (Lönnberg 1906) From the Palmer Archipelago (Southern Ocean) for Breeding Purposes." *Polar Biology* 40: 2499–2516.

Liu, J., A. Zhu, X. Wang, X. Zhou, and L. Chen. 2024. "Predicting the Current Fishable Habitat Distribution of Antarctic Toothfish (*Dissostichus mawsoni*) and Its Shift in the Future Under Climate Change in the Southern Ocean." *PeerJ* 12: e17131.

Love, M. I., W. Huber, and S. Anders. 2014. "Moderated Estimation of Fold Change and Dispersion for RNA-Seq Data With DESeq2." *Genome Biology* 15: 550.

Martin, B. T., P. N. Dudley, N. S. Kashef, et al. 2020. "The Biophysical Basis of Thermal Tolerance in Fish Eggs." *Proceedings of the Royal Society B: Biological Sciences* 287: 20201550.

Martin, B. T., A. Pike, S. N. John, et al. 2017. "Phenomenological vs. Biophysical Models of Thermal Stress in Aquatic Eggs." *Ecology Letters* 20: 50–59.

Martin, M. 2011. "Cutadapt Removes Adapter Sequences From High-Throughput Sequencing Reads." *EMBnet.Journal* 17: 10–12.

Martin, R. A., C. R. B. da Silva, M. P. Moore, and S. E. Diamond. 2023. "When Will a Changing Climate Outpace Adaptive Evolution?" *Wiley Interdisciplinary Reviews: Climate Change* 14: e852.

Meredith, M. P., and J. C. King. 2005. "Rapid Climate Change in the Ocean West of the Antarctic Peninsula During the Second Half of the 20th Century: Rapid Ocean Climate Change at the WAP." *Geophysical Research Letters* 32: L19604.

Miller, T. J., L. B. Crowder, J. A. Rice, and E. A. Marschall. 1988. "Larval Size and Recruitment Mechanisms in Fishes: Toward a Conceptual Framework." *Canadian Journal of Fisheries and Aquatic Sciences* 45: 1657–1670.

Nielsen, J. M., L. A. Rogers, R. D. Brodeur, et al. 2021. "Responses of Ichthyoplankton Assemblages to the Recent Marine Heatwave and Previous Climate Fluctuations in Several Northeast Pacific Marine Ecosystems." *Global Change Biology* 27: 506–520.

Novillo, M., M. Elisio, E. Moreira, G. Macchi, and E. Barrera-Oro. 2024. "First Insights Into the Influence of Temperature on Reproduction in Antarctic Fish: The Case of *Notothenia coriiceps*." *Estuarine, Coastal and Shelf Science* 297: 108629.

O'Brien, K. M., W. Joyce, E. L. Crockett, M. Axelsson, S. Egginton, and A. P. Farrell. 2021. "Resilience of Cardiac Performance in Antarctic Notothenioid Fishes in a Warming Climate." *Journal of Experimental Biology* 224: jeb220129.

Orsi, A. H., I. I. I. Whitworth, and J. Nowlin. 1995. "On the Meridional Extent and Fronts of the Antarctic Circumpolar Current." *Deep Sea Research. Part I. Oceanographic Research Papers* 42: 641–673.

Palmer Station Antarctica, L. T. E. R., and O. Schofield. 2025. Chlorophyll determined by extraction of samples taken approximately weekly from seawater intake starting at Palmer Station by station personnel including during winter-over period, 1991-2024 https://doi.org/10.6073/pasta/2c53e4542dddbf5e54269793ffaafc4a. ver 9. Environmental Data Initiative.

Papetti, C., H. S. Windisch, M. la Mesa, M. Lucassen, C. Marshall, and M. D. Lamare. 2016. "Non-Antarctic Notothenioids: Past Phylogenetic History and Contemporary Phylogeographic Implications in the Face of Environmental Changes." *Marine Genomics* 25: 1–9.

Peck, L. S. 2005. "Prospects for Survival in the Southern Ocean: Vulnerability of Benthic Species to Temperature Change." *Antarctic Science* 17: 497–507.

Peck, L. S. 2011. "Organisms and Responses to Environmental Change." *Marine Genomics* 4: 237–243.

Peck, L. S. 2023. "Responding to Warming in Polar Oceans: A Commentary on Molina et al. (2022)." *Global Change Biology* 29: 5–6.

Permitin, Y. E. 1977. "Species Composition and Zoogeographical Analysis of the Bottom Fish Fauna of the Scotia Sea." *Journal of Ichthyology* 17: 710–726.

Perry, F. A., S. Kawaguchi, A. Atkinson, et al. 2020. "Temperature–Induced Hatch Failure and Nauplii Malformation in Antarctic Krill." *Frontiers in Marine Science* 7: 501.

Pertea, M., G. M. Pertea, C. M. Antonescu, T. C. Chang, J. T. Mendell, and S. L. Salzberg. 2015. "StringTie Enables Improved Reconstruction of a Transcriptome From RNA-Seq Reads." *Nature Biotechnology* 33: 290–295.

Pimentel, M. S., F. Faleiro, G. Dionísio, et al. 2014. "Defective Skeletogenesis and Oversized Otoliths in Fish Early Stages in a Changing Ocean." *Journal of Experimental Biology* 217: 2062–2070.

Pimentel, M. S., F. Faleiro, T. Marques, et al. 2016. "Foraging Behaviour, Swimming Performance and Malformations of Early Stages of Commercially Important Fishes Under Ocean Acidification and Warming." *Climatic Change* 137: 495–509.

Pörtner, H.-O., C. Bock, and F. C. Mark. 2017. "Oxygen- and Capacity-Limited Thermal Tolerance: Bridging Ecology and Physiology." *Journal of Experimental Biology* 220: 2685–2696.

Postlethwait, J. H., Y. L. Yan, T. Desvignes, et al. 2016. "Embryogenesis and Early Skeletogenesis in the Antarctic Bullhead Notothen, *Notothenia coriiceps*." *Developmental Dynamics* 245: 1066–1080.

Ratnarajah, L., R. Abu-Alhaija, A. Atkinson, et al. 2023. "Monitoring and Modelling Marine Zooplankton in a Changing Climate." *Nature Communications* 14: 564.

Ready, J., K. Kaschner, A. B. South, et al. 2010. "Predicting the Distributions of Marine Organisms at the Global Scale." *Ecological Modelling* 221: 467–478.

Réalis-Doyelle, E., A. Pasquet, D. De Charleroy, P. Fontaine, and F. Teletchea. 2016. "Strong Effects of Temperature on the Early Life Stages of a Cold Stenothermal Fish Species, Brown Trout (*Salmo trutta* L.)." *PLoS One* 11: e0155487.

Robinson, M. D., and A. Oshlack. 2010. "A Scaling Normalization Method for Differential Expression Analysis of RNA-Seq Data." *Genome Biology* 11: R25.

Rodríguez-Romero, A., M. D. Jarrold, G. Massamba-N'Siala, J. I. Spicer, and P. Calosi. 2016. "Multi-Generational Responses of a Marine Polychaete to a Rapid Change in Seawater pCO_2." *Evolutionary Applications* 9: 1082–1095.

Rombough, P. J. 2023. "Respiratory Gas Exchange, Aerobic Metabolism, and Effects of Hypoxia During Early Life." *Fish Physiology* 40: 567–668.

Saleem, S., and S. C. Biswas. 2017. "Tribbles Pseudokinase 3 Induces Both Apoptosis and Autophagy in Amyloid-β-Induced Neuronal Death." *Journal of Biological Chemistry* 292: 2571–2585.

Sapota, M. R. 1999. "Gonad Development and Embryogenesis of *Notothenia coriiceps* From South Shetlands—Antarctica." *Polar Biology* 22: 164–168.

Saravia, J., K. Paschke, R. Oyarzún-Salazar, C. H. C. Cheng, J. M. Navarro, and L. Vargas-Chacoff. 2021. "Effects of Warming Rates on Physiological and Molecular Components of Response to CTMax Heat Stress in the Antarctic Fish *Harpagifer antarcticus*." *Journal of Thermal Biology* 99: 103021.

Schneider, C. A., W. S. Rasband, and K. W. Eliceiri. 2012. "NIH Image to ImageJ: 25 Years of Image Analysis." *Nature Methods* 9: 671–675.

Schulte, P. M. 2015. "The Effects of Temperature on Aerobic Metabolism: Towards a Mechanistic Understanding of the Responses of Ectotherms to a Changing Environment." *Journal of Experimental Biology* 218: 1856–1866.

Shin, S. C., D. H. Ahn, S. J. Kim, et al. 2014. "The Genome Sequence of the Antarctic Bullhead Notothen Reveals Evolutionary Adaptations to a Cold Environment." *Genome Biology* 15: 468.

Sidell, B. D., and K. M. O'Brien. 2006. "When Bad Things Happen to Good Fish: The Loss of Hemoglobin and Myoglobin Expression in Antarctic Icefishes." *Journal of Experimental Biology* 209: 1791–1802.

Smith, R. C., R. Smith, K. Baker, et al. 1995. "The Palmer LTER: A Long-Term Ecological Research Program at Palmer Station, Antarctica." *Oceanography* 8: 77–86.

Sokolova, I. 2021. "Bioenergetics in Environmental Adaptation and Stress Tolerance of Aquatic Ectotherms: Linking Physiology and Ecology in a Multi-Stressor Landscape." *Journal of Experimental Biology* 224: jeb236802.

Somero, G. N., and A. L. DeVries. 1967. "Temperature Tolerance of Some Antarctic Fishes." *Science* 156: 257–258.

Somero, G. N., B. L. Lockwood, and L. Tomanek. 2016. *Biochemical Adaptation: Response to Environmental Challenges, From Life's Origins to the Anthropocene*. Palgrave Macmillan.

Soneson, C., M. I. Love, and M. D. Robinson. 2015. "Differential Analyses for RNA-Seq: Transcript-Level Estimates Improve Gene-Level Inferences." *F1000Res* 4: 1521.

Stanwell-Smith, D., and L. S. Peck. 1998. "Temperature and Embryonic Development in Relation to Spawning and Field Occurrence of Larvae of Three Antarctic Echinoderms." *Biological Bulletin* 194: 44–52.

Suckling, C. C., M. S. Clark, J. Richard, et al. 2015. "Adult Acclimation to Combined Temperature and pH Stressors Significantly Enhances Reproductive Outcomes Compared to Short-Term Exposures." *Journal of Animal Ecology* 84: 773–784.

Swart, N. C., J. N. S. Cole, V. V. Kharin, et al. 2019. "CCCma CanESM5 Model Output Prepared for CMIP6 ScenarioMIP." https://doi.org/10.22033/ESGF/CMIP6.1317.

Vastenhouw, N. L., W. X. Cao, and H. D. Lipshitz. 2019. "The Maternal-To-Zygotic Transition Revisited." *Development* 146: dev161471.

Warkentin, K. M. 2011. "Environmentally Cued Hatching Across Taxa: Embryos Respond to Risk and Opportunity." *Integrative and Comparative Biology* 51: 14–25.

White, M. G., and P. J. Burren. 1992. "Reproduction and Larval Growth of *Harpagifer antarcticus* Nybelin (Pisces, Notothenioidei)." *Antarctic Science* 4: 421–430.

White, M. G., A. W. North, E. I. Twelves, and S. Jones. 1982. "Early Development of *Notothenia neglecta* From the Scotia Sea, Antarctica." *Cybium* 6: 43–51.

Wieser, W., and G. Krumschnabel. 2001. "Hierarchies of ATP-Consuming Processes: Direct Compared With Indirect Measurements, and Comparative Aspects." *Biochemical Journal* 355: 389–395.

Wu, T., E. Hu, S. Xu, et al. 2021. "clusterProfiler 4.0: A Universal Enrichment Tool for Interpreting Omics Data." *Innovation (Camb.)* 2: 100141.

Yu, G., L.-G. Wang, Y. Han, and Q.-Y. He. 2012. "clusterProfiler: An R Package for Comparing Biological Themes Among Gene Clusters." *OMICS* 16: 284–287.

Supporting Information

Additional supporting information can be found online in the Supporting Information section. **Figure S1:** Schematic of vertical incubator system. Seawater entering the Palmer Station Aquarium header tanks was sterilized using a UV light source, and oxygen saturation was maintained with air pumps and spargers. The experimental tank's seawater temperature was regulated at 4.0°C ± 0.2°C using feedback-controlled submersible heaters. The controlled temperature room was maintained at 2°C to keep the control (0°C) seawater near ambient conditions. Seawater flowed to both reservoir tanks and vertical incubators; however, conical jars were not used due to overflow issues but remained connected to the system. Temperature loggers recorded tank temperatures at hourly intervals. Annotations indicate the placement of drawers used for technical replicates. **Figure S2:** Design of technical replicates. Embryos from four natural, mixed parentage spawns were combined and divided into two incubator drawers (486 g in each). Embryos remained in these incubator drawers until 15 dpf, when half of the embryos were removed from each drawer and moved into large beakers in upright incubators (243 g from each replicate tray). The temperature of each upright incubator was raised by one degree per day for 4 days. At 19 dpf, the embryos from each beaker were placed into two drawers in the heated vertical incubator (Figure S1). **Figure S3:** Daily incubation temperatures. Temperatures were recorded hourly using submersed temperature data loggers. Points represent the daily average temperature measured from the bottom drawer of each incubator. The gray dashed line marks 15 dpf, when embryos were removed for a slow temperature ramp to the heated condition (4°C). The red dashed line denotes 19 dpf, when heated embryos were transferred to the heated incubator. Trend lines represent a linear model fitted to each dataset with confidence bands (lm, geom_smooth). The black star at 84 dpf indicates a temperature drop anomaly caused by a malfunction in the flow switch, which temporarily disrupted the heating elements. Temperature was gradually ramped back up by 1°C per day until reaching 4°C. **Figure S4:** Subtle difference in mortality due to temperature. (A) Percent survival over incubation time, including a mortality event in ambient 2 at 40 dpf. An estimated 1800 embryos died for an unknown reason. However, after this, there was minimal mortality seen during incubation. (B) Percent survival starting from after the mortality event. A slight impact of heat on mortality can be seen, but values were mostly stable, indicating only a subtle difference in mortality due to temperature. **Figure S5:** Segmentation and eye iridescence in 0°C and 4°C hatchlings. The embryo for ambient eye iridescence was dechorionated before the photograph was taken. All other embryos are micrographed with their chorions intact. Note that the micrographs for the eye iridescence embryos were recorded near, but not on, the nominal dates for this stage that are reported in the text. **Figure S6:** Growth of *N. coriiceps* embryos. Total lengths of embryos reared at 0°C and 4°C through hatching. Each point represents the length of one randomly sampled embryo; the same embryos were not followed through development. Confidence bands around linear trendlines represent 98% confidence intervals. Slope of 4°C line is 0.13 mm/day, slope of 0°C line is 0.1 mm/day. Black arrows represent the onset of hatching for each treatment group. **Figure S7:** Heatmap of sample distances determined by DESeq2 (v.1.46.0). Samples clustered by developmental stage rather than treatment, indicating consistent gene expression patterns across this morphology-based sampling strategy. Ambient refers to ambient water temperatures (0°C), elevated refers to 4°C. The analyzed stages are the onset of heartbeat (HB), 50% eye pigmentation (EP), eye iridescence (EI), and hatching (H). Days post-fertilization (d) are listed for each sample. **Table S1:** Timing of developmental stages in 0°C and 4°C treatments. **Table S2:** Measurements and deformity classification of late embryos and hatchlings in 0°C and 4°C treatments. See supporting attachments for spreadsheet. **Table S3:** Differential expression between treatments of all genes at all stages as reported by DESeq2 v.1.46.0. See supporting attachments for spreadsheet. **Table S4:** GO enrichment data for all stages. NAs represent terms where no genes were significantly differentially expressed. See supporting attachments for spreadsheet. **Table S5:** Oxygen saturation in bottom tray of 0°C and 4°C drawer incubators. **Table S6:** Alignment statistics as reported by Cutadapt v1.18 and HiSat2 v.2.2.1. See supporting attachments for spreadsheet.